

Multilayer structure enhances the optimal outcome of coordination games

Tomasz Raducha^{1,2,*} and Maxi San Miguel¹

¹Grupo Interdisciplinar de Sistemas Complejos (GISC), Departamento de Matemáticas, Universidad Carlos III de Madrid, Leganés, Spain

²Instituto de Física Interdisciplinar y Sistemas Complejos IFISC (CSIC-UIB), Palma, Spain

*tjan@math.uc3m.es

ABSTRACT

We study mechanisms of synchronisation, coordination, and equilibrium selection in two-player coordination games on multilayer networks. We apply the approach from evolutionary game theory with three possible update rules: the replicator dynamics (RD), the best response (BR), and the unconditional imitation (UI). Players interact on a two-layer random regular network. The population on each layer plays a different game, with layer I preferring the opposite strategy to layer II. We measure the difference between the two games played on the layers by a difference in payoffs ΔS while the inter-connectedness is measured by a node overlap parameter q . We discover a critical value $q_c(\Delta S)$ below which layers do not synchronise. For $q > q_c$ in general both layers coordinate on the same strategy. Surprisingly, there is a symmetry breaking in the selection of equilibrium – for RD and UI there is a phase where only the payoff-dominant equilibrium is selected. Our work is an example of previously observed differences between the update rules on a single network. However, we took a novel approach with the game being played on two inter-connected layers. As we show, the multilayer structure enhances the abundance of the Pareto-optimal equilibrium in coordination games with imitative update rules.

Introduction

Spontaneous emergence of coordination between people or animals, without external control, is a remarkable phenomenon that can be crucial for optimal functioning or even survival of the population^{1–3}. In some circumstances individuals are facing a choice between two or more possible actions, called strategies, they can take. It often happens that the best outcome for everyone can be obtained only if we choose the same strategy as our neighbours. In game theory such situation is referred to as coordination game^{4–7}. Additionally, it might matter under which strategy the population coordinates. One action can lead to higher prosperity than the other, what is modelled by different strategies having different payoffs. Conditions required to coordinate have been scrutinised under various assumptions and for numerous environments, yet there are still unanswered questions. Here, we study coordination and equilibrium selection in games on multilayer networks.

People interact in multiple contexts and through different media. One of natural ways to represent it in a strict manner is by using a multilayer network^{8–12}. Each layer is a separate network of interactions in a given context. For example, we interact with each other in work place, at home, online etc. In principle, the pattern of interactions can be different in every layer resulting in a different network topology. Additionally, some layers can be hidden¹³. Not every person must be active in every environment, therefore some nodes are present only on a specific layer. If a node exists in many layers, however, it represents the same person, which often acts similarly in every context. It is therefore connected between layers to itself via inter-layer links, which provide coupling between the layers. It is important to note that, if a system has a multilayer structure, it can not be simply reduced to a single-layer graph without changing the dynamics¹⁴. Hence, the scrutiny of layered systems is highly relevant.

We use the approach from evolutionary game theory^{15–18} to analyse synchronisation between the layers and equilibrium selection in coordination games. Coordination games have been studied in depth on single layer networks, a comprehensive literature review can be found here¹⁹. From previous results it is worth mentioning the KMR model which explored the equilibrium selection in populations equivalent to complete graphs with the best response update rule²⁰. The risk-dominant equilibrium was always evolutionary favoured in the model and several extensions did not find any deviation from this behaviour^{21–24}. That outcome is preserved also on a circular network²⁵, unless the unconditional imitation is used to update strategies²⁶. In general, imitative update rules can favour Pareto-efficiency over risk dominance^{19,27,28}.

Evolutionary games were also extended to multilayer networks²⁹. Prisoner’s dilemma was studied on many layers with a possibility of using different strategies on different layers. The strategy was updated according to replicators dynamics, but using the collective payoff from all layers^{30,31}. It was also studied together with the stag hunt, the harmony game, and the snow

drift on two-layer networks with the game being played on one layer and strategy imitation on the other³². Additionally, the same games on one layer were mixed with opinion dynamics and social influence on the second layer³³. The idea of separating the group in which we play the game from the one where we learn or imitate the strategy had been already studied before within a single network^{34–37}. The public goods game^{38–40} was considered on two⁴¹ and more layers⁴² with the game being played on each layer. Interestingly, in some of the mentioned research the multilayer structure was said to enhance cooperation^{30,33,41}. Finally, coordination games were also investigated on multilayer networks. The pure coordination game on one layer was coupled with social dynamics and coevolution on the other, leading to a possible segregation⁴³. A particular version of the general coordination game was studied on a two interconnected layers, with the strategy being imitated on the layers and the game played between the layers^{44–46}. Similarly to single-layer networks, the unconditional imitation and smaller degree favoured the Pareto-optimal equilibrium. However, the body of work on coordination games on multilayer networks is still very limited and consists of particular cases of more complex models mixed with opinion dynamics. Moreover, different works consider different update rules and it is difficult to judge to which extent results are determined by the multilayer structure, the particular payoff matrix, or the chosen update rule. Comparison between different update rules is necessary. For these reasons, we provide a broader analysis of different payoff matrices laying within the coordination games scope together with three different update rules.

We focus on the two-player general coordination game¹⁹ described by a 2×2 payoff matrix:

$$\begin{array}{cc} & \begin{matrix} A & B \end{matrix} \\ \begin{matrix} A & \\ B & \end{matrix} & \begin{pmatrix} 1 & S \\ T & 0 \end{pmatrix} \end{array}, \quad (1)$$

where A and B are available strategies, while T and S are parameters defining payoffs. By definition, coordination games must fulfil conditions $T < 1$ and $S < 0$. Note that the payoff matrix (1) is equivalent to the most general one with all four payoffs defined by a parameter, if only coordination on the strategy A is more lucrative than on the strategy B. Without loss of generality we can reduce it to the presented form. A game described by such payoff matrix contains a social dilemma. Obviously, the most rewarding outcome is obtained if both players choose the same strategy, but there is a hidden trade off between security and profit. Clearly, the highest possible profit is made when both play the strategy A, hence it is called the payoff-dominant or Pareto-optimal strategy. On the other hand, the risk-dominant strategy is the best choice in the lack of knowledge, i.e. it is the strategy that results in the highest average payoff assuming that the opponent will play either way with the same probability⁴⁷. It is easy to check that for $T < S + 1$ the strategy A is risk-dominant, and for $T > S + 1$ the strategy B is be risk-dominant. This calculation provides a theoretical line $T = S + 1$ at which risk dominance changes. When all players coordinate on one of these strategies we refer to such state as a payoff-dominant or risk-dominant equilibrium.

In the evolutionary game theory the game evolves because the players update their strategies after interacting and observing their peers. It is well known that the update rule is as important as the payoff matrix in defining the end result of the game^{19,27,28,48–51}. Multiple update rules have been proposed in the literature^{52–55}. We focus on three well established ones: the replicator dynamics (RD)^{56–58}, the best response (BR)^{20,21,25,59–61}, and the unconditional imitation (UI)^{17,44–46,62,63}. It is important to note that RD and UI are imitative in nature, as players adapt the strategy of one of the neighbours. BR on the other hand is a strategical update rule which requires from the player knowledge about the payoff matrix. Another distinction between the update rules is their determinism – BR and UI are deterministic, meaning that the same configuration will always lead to the same strategy being chosen, while RD is a probabilistic update rule. See Methods section for more details.

It was shown that on a single-layer network the risk aversion is usually stronger than the drive to profit. Therefore, on complete graphs the risk-dominant equilibrium is always obtained. For sparse networks under unconditional imitation the system can favour the Pareto-optimal equilibrium over the risk-dominant one, but only for a limited range of parameters¹⁹. For RD and BR, however, the risk-dominant equilibrium is always selected. In general, local effects were shown to be more important for update rules which have an imitative nature, such as unconditional imitation^{26–28}. A natural question is which equilibrium, if any, will be chosen when the population is placed on a multilayer network with two layers on opposite sides of the $T = S + 1$ risk-dominance transition line. In other words, on layer I agents play a game where the strategy A is risk-dominant and on layer II a game where the strategy B is risk-dominant. We investigate it by means of numerical simulations.

We study a population of players participating in two games on a multilayer network with two inter-connected layers, as depicted in Figure 1. Both layers have the same number of nodes N . If a node is connected to itself between the layers via an inter-link, it plays the same strategy everywhere. The fraction of nodes connected (or shared) between the layers is controlled by a parameter $q \in [0, 1]$, called node overlap or degree of multiplexity^{14,64}. There are Nq inter-layer connections. For $q = 0$ the two layers are effectively two independent networks, for $q = 1$ the layers are equivalent to one network (every node is the same on each layer all the time) playing each game half of the times. The edge overlap is kept constant with both layers having the same topology, since we did not observe any change under varying edge overlap. We use random regular graphs⁶⁵. See Methods for more details on our simulations.

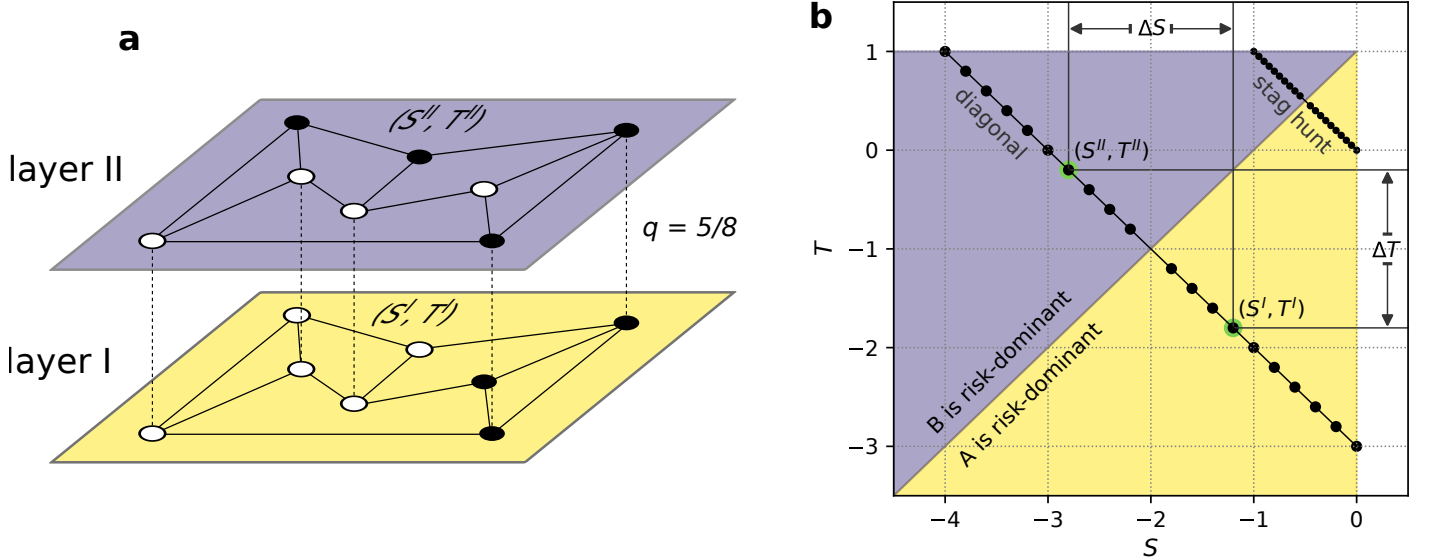


Figure 1. (a) Schematic representation of a miniature of multilayer network used in our simulations. Both layers have the same topology of a random regular graph with $N = 8$ nodes of degree $k = 3$ each and a fraction $q = 5/8$ of nodes is shared between the layers. Shared nodes are connected by inter-layer connections (dashed lines). The node overlap q is the number of shared nodes divided by N . White nodes play the strategy A and black ones play the strategy B. Shared nodes always have the same state on both layers. Each layer has a specific payoff matrix given by (S^I, T^I) and (S^{II}, T^{II}) . (b) Diagram of the S - T parameter space showing parametrisation of the layers. Each circle on the diagonal lines represents a game played on one of the layers. On layer I the strategy A is always risk-dominant (yellow area), and on layer II the strategy B is always risk-dominant (purple area). Risk-dominance changes at the line $T = S + 1$. Exemplary values of (S^I, T^I) and (S^{II}, T^{II}) are highlighted in green with ΔS and ΔT illustrated.

Players on each layer are engaged in different games, i.e. parameters S^β and T^β , $\beta \in \{I, II\}$, defining the payoff matrix have different values on each layer. In order to give the same relevance to both layers, their preferences towards one of the equilibria are set to be equally strong. This is achieved by choosing the points (S^I, T^I) and (S^{II}, T^{II}) equally distant from the $T = S + 1$ line, as visible in Figure 1. Another choice to make is the angle between the $T = S + 1$ line and the line created by points (S^I, T^I) and (S^{II}, T^{II}) . We focus on cases where all points lay on a line $T^\beta = -S^\beta + C$, where C is a constant (see Supplementary Material for other cases). This is because only then the average payoffs $\langle \Pi^I \rangle$ and $\langle \Pi^{II} \rangle$ of both layers are equal, therefore games are truly symmetrical. We analyse the case of $T^\beta = -S^\beta - 3$, which we call *diagonal*, and $T^\beta = -S^\beta$ where all games are variants of the well known *stag hunt*^{66,67}. Note, that the *stag hunt* game can be obtained for different values of C and that both cases are „diagonal” in the sense that they have the same slope. Nevertheless, we call the case of $C = -3$ *diagonal* and $C = 0$ *stag hunt* to easily distinguish them in the discussion of results that follows in the manuscript. In both cases we cover with the parameters S and T the whole width of the general coordination game area (see Figure 1).

Since the layers are placed symmetrically around the $T = S + 1$ line, or more precisely around a point (S_0, T_0) at this line, the parameter $\Delta S = S^I - S^{II}$ is sufficient to determine values of all four parameters S^I, T^I, S^{II}, T^{II} . Namely:

$$\begin{aligned}
 S^I &= S_0 + \frac{\Delta S}{2}, \\
 T^I &= T_0 - \frac{\Delta T}{2}, \\
 S^{II} &= S_0 - \frac{\Delta S}{2}, \\
 T^{II} &= T_0 + \frac{\Delta T}{2},
 \end{aligned} \tag{2}$$

where $(S_0, T_0) = (-2, -1)$ for the diagonal case and $(S_0, T_0) = (-0.5, 0.5)$ for the *stag hunt* case. Note also that for $T^\beta = -S^\beta + C$, that is both cases, we have $\Delta S = \Delta T$. We use the coordination rate $\alpha \in [0, 1]$ to describe the state of the population. When $\alpha^\beta = 1$ every player on the layer β chooses the strategy A, therefore layer β is in the Pareto-optimal equilibrium. When

$\alpha^\beta = 0$ the layer also coordinates, but on the strategy B. For $\alpha^\beta = 0.5$ both strategies are mixed in equal amounts in the layer β . We say that the layers are synchronised when $\alpha^I = \alpha^{II}$ and then we use just α to describe both of them. Note that synchronisation does not require coordination within the layers and vice versa, although they usually come together in our results.

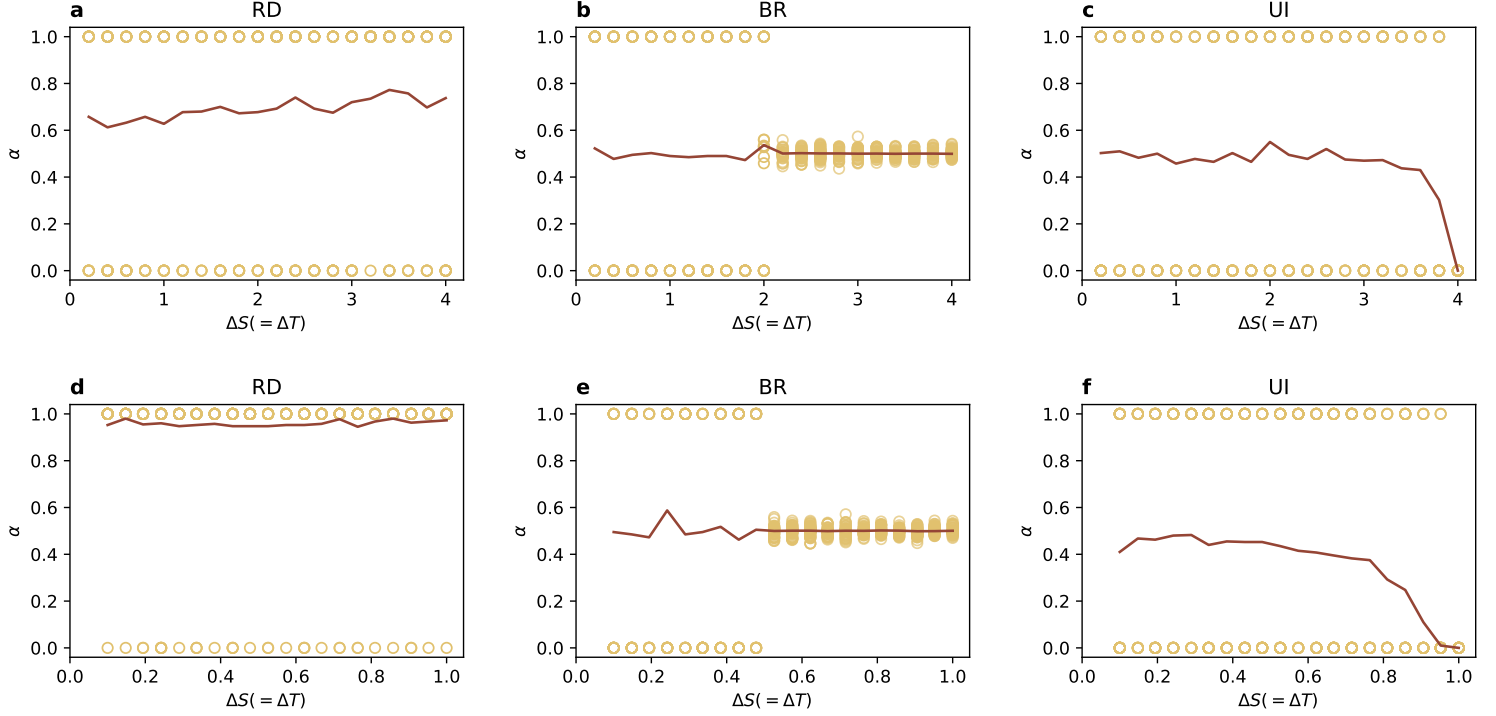


Figure 2. Coordination rate $\alpha = \alpha^I = \alpha^{II}$ vs gap size ΔS for full node overlap $q = 1$ (the multiplex case). The upper row (a, b, c) presents the diagonal case and the bottom row (d, e, f) the stag hunt. For RD and BR each layer has $N = 1000$ nodes with an intra-layer degree $k = 8$, for UI it is a complete graph with $N = 500$. Each circle represents the value of α (for both layers) in one of 400 realisations and solid lines show the average values.

Results

We study the synchronisation between the layers, coordination, and equilibrium selection under varying conditions. For RD and BR update rules we set the connectivity at $k = 8$, since it was shown that the degree does not change the equilibrium selection in their case¹⁹. However, for UI the line $T = S + 1$, at which risk-dominance of strategies changes, overlaps with the actual transition in equilibrium selection only for a complete graph¹⁹. Hence, we analyse the case of unconditional imitation always with full connectivity in order to obtain true symmetry between the layers.

The two main parameters whose influence we investigate are the node overlap q and the distance between the games ΔS or ΔT . For simplicity, we start with an analysis of the multiplex case, i.e. full node overlap, $q = 1$. In Figure 2 we present the coordination rate α for synchronised layers at $q = 1$ (layers are always synchronised at full node overlap, because all nodes have to be the same on both layers by definition). The RD update rule clearly favours the payoff-dominant strategy A at the maximal level of multiplexity. In the diagonal case the difference is moderate with $0.6 \lesssim \alpha \lesssim 0.8$, but in the stag hunt case coordination rarely happens at the strategy B and α is close to 1.

Interestingly, for $q = 1$ the UI update rule does not favour the strategy A. As we can see in the figure, for small size of the gap ΔS the outcome is symmetrical with both strategies selected half of the time. But for increasing distance between the layers the system starts to coordinate more often on the strategy B, to finally select exclusively the not Pareto-optimal equilibrium for the maximal gap size. It has to be noted that the maximal gap size results in payoff matrices that are on the border between coordination games area and non-coordination games, therefore this very point technically does not represent a coordination game. Nonetheless, the decline in the payoff-dominant equilibrium selection is visible already before this limit value. This result is especially surprising, since the UI is the only update rule that on a single-layer network can lead to the Pareto-optimal equilibrium even though it is not risk-dominant¹⁹. However, the requirement for that was a sparse network.

The only truly symmetric update rule is the BR which does not reveal any preference towards one of the strategies for full node overlap. Additionally, the diagonal case is identical to the stag hunt case. For gaps $\Delta S < \Delta S_{max}/2$ and $q = 1$ synchronised layers reach either equilibrium with equal probability, and for $\Delta S > \Delta S_{max}/2$ the system does not coordinate staying at $\alpha = 0.5$. At the transition value of $\Delta S = \Delta S_{max}/2$ both states – the coordination on one of the strategies and non-coordinated fully-mixing state – are possible (see Figure 2).

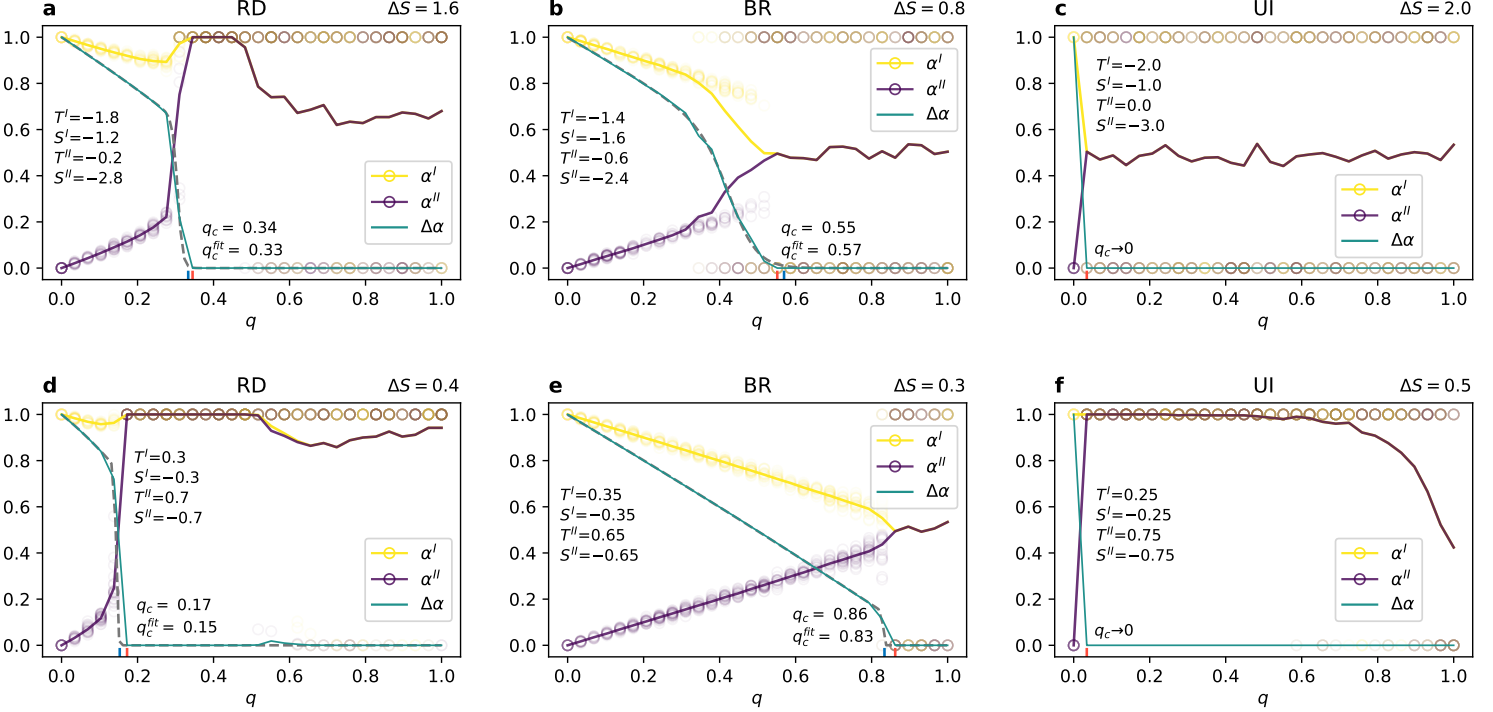


Figure 3. Coordination rates on layers α^I , α^{II} , and $\Delta\alpha$ vs node overlap q for exemplary values of ΔS . The upper row (a, b, c) presents the diagonal case and the bottom row (d, e, f) the stag hunt. For RD and BR each layer has $N = 1000$ nodes with an intra-layer degree $k = 8$, for UI it is a complete graph with $N = 500$. Each circle represents one of 500 realisations and solid lines show the average values. For each realisation there is one circle for layer I (yellow) and one for layer II (purple). Note, that when layers synchronise $\alpha^I = \alpha^{II}$, $\Delta\alpha = 0$, and both circles overlap looking like one of brownish colour, as well as the solid lines for α^I and α^{II} merge. The dashed line in (a, b, d, e) shows the function fitted to $\Delta\alpha$.

In addition to the results showed in Figure 2 for $q = 1$, we know that for $q = 0$ each layer will obtain full coordination on its preferred strategy – A for layer I and B for layer II¹⁹. The middle ground between those two extreme values of q must therefore contain some kind of transition. We investigate it in Figure 3, where we can see how the coordination rate α changes at both layers with increasing q . First thing to notice is that for any update rule and any parameter choice, but with $q = 0$, each layer converges to a different limit value of α . This means that both layers indeed obtain full coordination on their preferred strategies. Consequently, the difference between layers is maximal and $\Delta\alpha = 1$. Such outcome was to be expected, because with no inter-connections the two layers are effectively separate networks, as we described. Therefore, each network selects the risk-dominant equilibrium. Similarly, for $q = 1$ layers must fully overlap with $\Delta\alpha = 0$, because each node is present on all layers and the state of a shared node must be the same across the layers. As visible in Figure 3 this is exactly what happens.

The above considerations lead to a conclusion that there must be a certain point $q_c \in [0, 1]$ at which $\Delta\alpha$ becomes zero. In Figure 3 we see that the value of q_c can vary for replicator dynamics and best response update rules, but is close to zero in both cases for unconditional imitation. In fact, $q_c \rightarrow 0$ for any configuration of the layers when players update their strategies according to UI (see Supplementary Materials for plots of different cases). In other words, synchronisation between the layers is the strongest for the UI update rule. One has to still bear in mind that for UI the network has a higher degree than in other cases. It is a complete graph, whereas for RD and BR the networks are much sparser with $k = 8$. Nevertheless, simulations for higher degree for BR indicate that synchronisation is weakened by increasing connectivity (see Supplementary Materials), which makes the update rule a natural explanation of the observed differences.

Another surprising observation is that not all the results are symmetrically placed around $\alpha = 0.5$. Both layers have equally

strong preferences towards their natural equilibria – payoff matrix parameters (S^I, T^I) and (S^{II}, T^{II}) are equally distant from the transition line $T = S + 1$ and average payoffs of the games on both layers are the same. There is no reason, in principle, why the system as a whole should choose one equilibrium over the other. Nevertheless, we can see that in some cases with RD and UI synchronised layers coordinate exclusively on the Pareto-optimal strategy A ($\alpha = 1$), while it doesn't happen for the strategy B at any point (except for $q = 1$ with the maximal gap ΔS for UI, see Figure 2). This symmetry breaking is especially interesting, because it is driven by the level of multiplexity q in a non-trivial way. In examples shown in Figure 3, and in general, if the Pareto-optimal equilibrium is obtained on both layers it happens as soon as they synchronise, i.e. at q_c . When increasing the node overlap further at some point q_p the synchronised state with coordination on the strategy B starts to appear and the average value of α drops below 1. For $q > q_p$ synchronised layers can coordinate on either strategy, however $\alpha > 0.5$ most of the time meaning that the Pareto-optimal equilibrium is still dominant.

The fully symmetrical outcome that one would expect from the symmetrical design of the experiment is obtained solely for BR. We can see in Figure 3 that there are only two types of behaviour that the system displays with BR update. The first one, for $q < q_c$ is characterised by no synchronisation between the layers and each of them following a specific level of coordination, which is $\alpha^I = -q/2 + 1$ and $\alpha^{II} = q/2$. This calculation comes from a simple assumption that all nodes that are not shared play the dominant strategy of their layer and all shared nodes play either strategy half of the time. Put differently, half of the shared nodes play the strategy A and half the strategy B. This gives a fraction $(1-q) + q/2 = -q/2 + 1$ of nodes playing the strategy A on the layer I and the same fraction of nodes playing the strategy B on layer II, so $1 - (-q/2 + 1)$ of them playing the strategy A. As we can see in the figure this scenario is realised until reaching q_c . The second type of behaviour, for $q > q_c$, is coordination of both synchronised layers on one of the strategies with equal probability of choosing either of them.

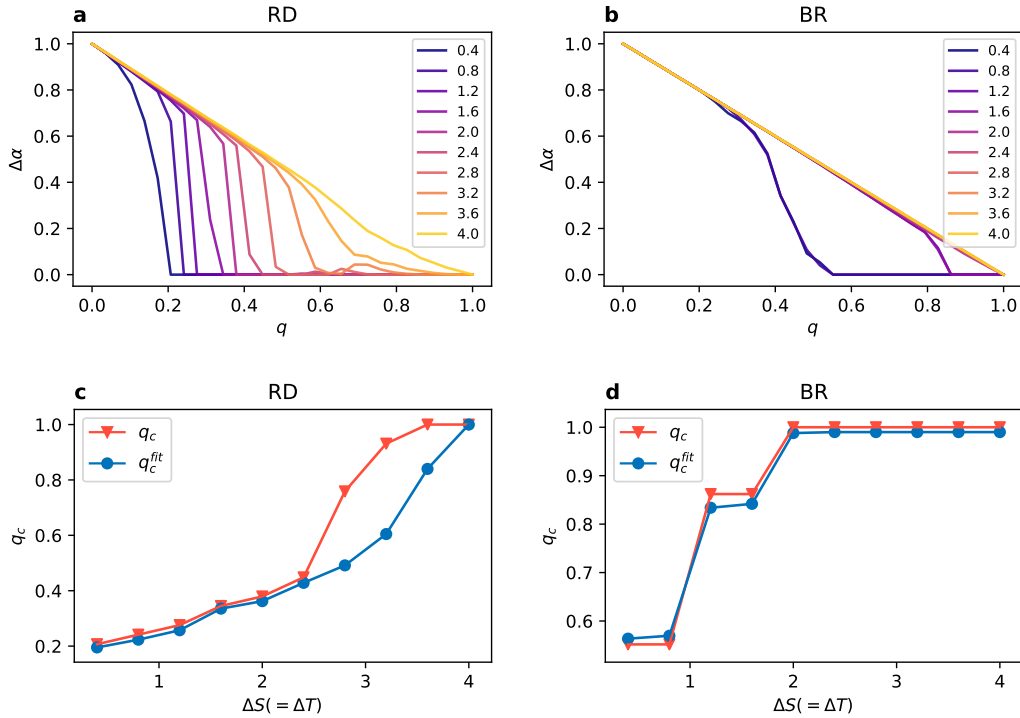


Figure 4. (a, b) Coordination rate difference between the layers $\Delta\alpha$ vs node overlap q for increasing value of ΔS (given in the legend). (c, d) Critical value of q_c and q_c^{fit} vs gap size ΔS . Results for the diagonal case, $N = 1000$ nodes on each layer with an intra-layer degree $k = 8$ averaged over 100 realisations.

The behaviour observed so far leads to a logical question about the change, if any, we would observe when varying the distance between the layers, i.e. for different values of the gap size ΔS . In Figures 4 and 5 (a, b) we present the dependence of $\Delta\alpha$ on the degree of multiplexity q for values of ΔS ranging from 0.4 to 4 in the diagonal case, and from 0.1 to 1 for the stag hunt. This range essentially covers the whole width of the general coordination game's scope. What we can see is that $\Delta\alpha$ drops to zero at higher node overlap when increasing the gap size. More precisely, for RD it roughly follows the line of $\Delta\alpha = -q + 1$ to diverge from it at some point and eventually reach the lowest possible value of 0. The line is followed for much longer in the diagonal case

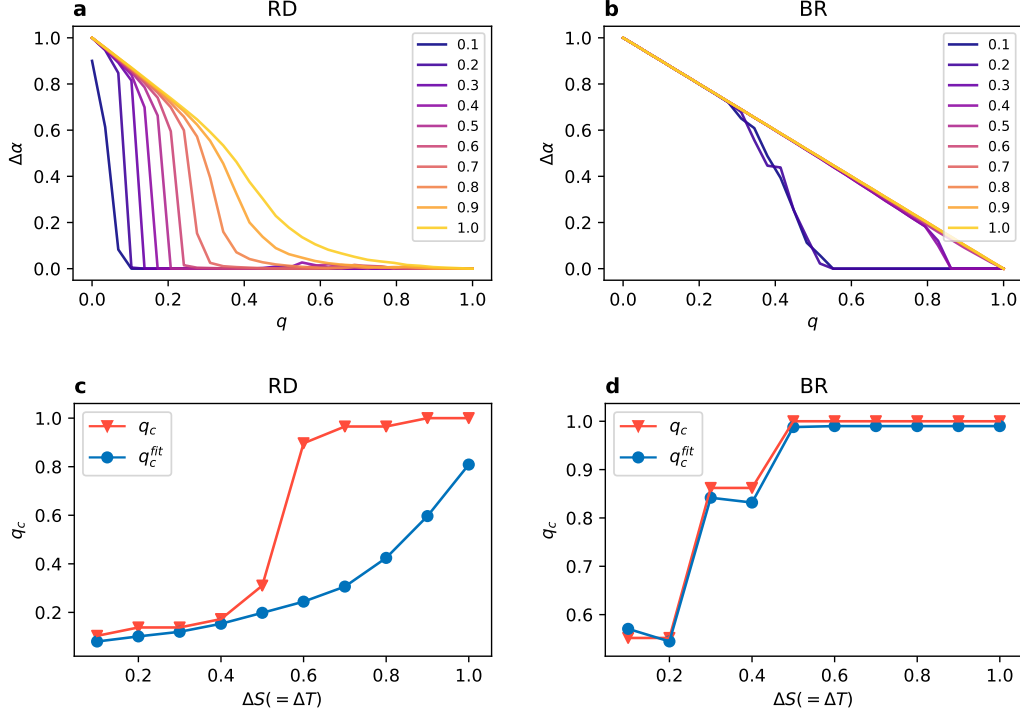


Figure 5. (a, b) Coordination rate difference between the layers $\Delta\alpha$ vs node overlap q for increasing value of ΔS (given in the legend). (c, d) Critical value of q_c and q_c^{fit} vs gap size ΔS . Results for the stag hunt case, $N = 1000$ nodes on each layer with an intra-layer degree $k = 8$ averaged over 100 realisations.

than in the stag hunt case. For BR there is virtually no difference between those cases and the dependence on the gap size is slightly different. Values of $\Delta\alpha$ are the same for gap sizes equal 0.4 and 0.8, then again for 1.2 and 1.6, and from $\Delta S = 2$ onwards $\Delta\alpha = -q + 1$ (these values are for the diagonal case, for stag hunt the general picture is the same with values rescaled by a factor of 1/4).

We can clearly see that q_c depends on the gap size ΔS and this dependence is presented in Figures 4 and 5 (c, d). We use two approaches in order to estimate the value of q_c . The first one is simply taking the lowest value of q at which $\Delta\alpha$ is equal 0 for the first time. This approach, however, is prone to numerical noise and a tiny divergence from 0 will result in a change of the value. To obtain the second one we fit a parabola with an exponential cutoff to the function $\Delta\alpha(q)$ (dashed line in Figure 3) and we take the first value of q at which $\Delta\alpha < 0.01$ as q_c^{fit} . As we can see in the plots, it does not make a real difference for BR, but can give different results for RD for higher values of ΔS . Regardless the approach, q_c changes from approximately 0.2 up to 1 for RD in the diagonal case (for the stag hunt values are slightly lower), and from 0.5 to 1 for BR with no visible difference between the diagonal and the stag hunt case. We similarly estimate the value of q_p , however without fitting a function, because the behaviour of α for synchronised layers is more complex than the one of $\Delta\alpha$. We take as an approximation of q_p the first value of q after synchronisation for which the coordination rate α drops below 0.95 (dashed lines in Figure 6).

In summary, for any gap ΔS (or ΔT) between the layers at $q = 0$ there is no synchronisation and each layer gravitates towards its preferred equilibrium. Then, at $q = q_c$ layers start to synchronise. For RD and UI synchronised layers coordinate on the Pareto-optimal strategy for $q_c < q < q_p$ and for $q > q_p$ they coordinate on either of the strategies. For some values of ΔS , however, as well as for BR in general, q_p overlaps with q_c and the system goes from unsynchronised state straight into coordination on any strategy, without the phase of pure Pareto-optimal equilibrium (see Figure 6). Additionally, there are two update-rule-specific phenomena. For UI at the maximal gap between the layers ($\Delta S_{max} = 4$ for the diagonal case and $\Delta S_{max} = 1$ for the stag hunt) and for $q = 1$ synchronised layers coordinate only on the strategy B just at this point. And for BR for $\Delta S > \Delta S_{max}/2$ at full node overlap when the layers get synchronised they do not reach coordination. Instead they both end up in a fully mixing state with $\alpha^I = \alpha^{II} = 0.5$.

We can also see from Figure 6 that an increase in the absolute values of payoffs S^β and T^β on both layers, i.e. a shift from the diagonal to the stag hunt case, significantly enlarges the relative area of Pareto-optimal equilibrium for RD and UI. It does not, however, change the relative size of the no-synchronisation phase and it seems not to influence the best response dynamics

at all. One explanation of the enlargement of the Pareto-optimal phase, at least for RD, could be the fact that in the stag hunt case the layers are closer to each other – the gap ΔS (and ΔT) is 4 times smaller on average. Games being more similar and closer to the transition line could justify why it is easier for the layer I to shift the layer II into its preferred equilibrium on the strategy A. Nevertheless, for UI in the diagonal case there is a minimal value $\Delta S \approx 2$ below which the Pareto-optimal phase does not exist at all, hence here the proximity of layers can not be the explanation of synchronisation in the payoff-dominant equilibrium. Moreover, there is an optimal size of the gap ΔS for which the Pareto-optimal phase is the widest. For UI it is approximately the maximal gap ΔS_{max} and for RD it is one of the middle values, but certainly not the smallest gap. These considerations lead us to a conclusion that synchronisation and equilibrium selection in coordination games on multilayer networks are very complex phenomena where obtaining the most advantageous outcome requires accurate parameter selection.

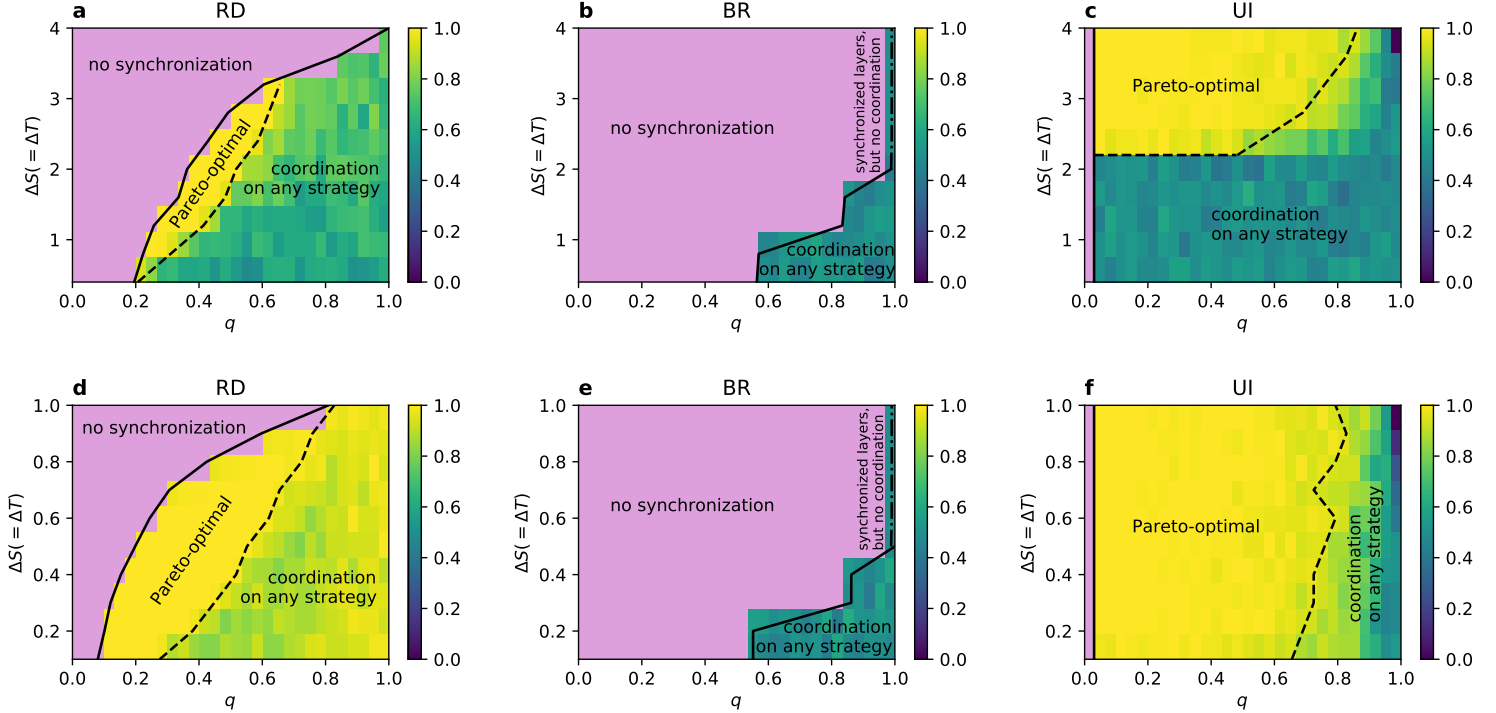


Figure 6. Phase diagram of coordination rate $\alpha = \alpha^I = \alpha^{II}$ in the q - ΔS space, for synchronised layers for the diagonal (a, b, c) and the stag hunt (d, e, f) case. The pink area represents the range of parameters where synchronisation is not obtained and $\alpha^I \neq \alpha^{II}$ (for UI it happens only at $q = 0$). The solid lines show the critical value q_c^{fit} and the dashed lines q_p . For RD and BR each layer has $N = 1000$ nodes with an intra-layer degree $k = 8$, for UI it is a complete graph with $N = 500$. Results are averaged over 100 realisations.

Discussion

We investigated synchronisation between layers and equilibrium selection in the general coordination game on a multilayer network. The game played on each layer is described by a different payoff matrix, but both games are equally distant from the risk-dominance transition line $T = S + 1$. The layers are connected by Nq inter-links, where the parameter q is the node overlap or degree of multiplexity. We studied the impact of the value of q and the gap ΔS between the layers for three update rules: the replicator dynamics, the best response, and the unconditional imitation.

The most prominent outcome is the symmetry breaking in equilibrium selection. In neither of the cases, diagonal and stag hunt, there is a difference in average payoffs of games played on the layers. The strategies preferred by each layer are equally risk-dominant, i.e. the distance from the transition line $T = S + 1$ is the same. The only difference, of course, is that the strategy A gives the highest possible payoff, hence it's the most profitable one. A common-sense approach would lead us to believe that the payoff-dominant strategy A should be naturally promoted by the population. This is however not the case on single-layer networks, where the risk-dominant strategy is always selected in the range of connectivities that we considered¹⁹. In our multilayer model, which strategy is risk-dominant depends on the layer, but coordination on the strategy A prevails in

most of the parameters space or is at least favoured on average. It is therefore clear that the multilayer structure enhances the Pareto-optimal outcome and it does so in a complex manner.

We identified three main phases depending on the node overlap q and the gap size ΔS . The first one for lower values of q is a no-synchronisation phase with $\alpha^I \neq \alpha^{II}$. Each layer obtains a certain level of coordination close to its preferred equilibrium. The second phase begins when $\Delta\alpha$ drops to zero, i.e. at q_c . Here, layers are synchronised and fully coordinate on the Pareto-optimal strategy A. Finally, the third phase appears for a higher node overlap $q > q_p$. In this phase layers are also synchronised and they also coordinate, but not always on the strategy A – either equilibrium is possible, although depending on the parameters one of them might be preferred on average. In some cases $q_c = q_p$ and the second phase does not appear.

The Pareto-optimal phase is not a mere effect of high node overlap between layers or low gap size. It has a more complex shape that depends on both parameters and on the update rule. For BR the Pareto-optimal phase does not exist at all. For RD it is placed, surprisingly, in the middle rage of the node overlap q , but its position and width depends also on ΔS . Neither too low nor too high degree of multiplexity helps in achieving the optimal equilibrium, and the same is true for the gap size. Nevertheless, the value of q_c grows with increasing distance ΔS . For UI the Pareto-optimal phase might not even exist for lower values of ΔS , and its usually wider for bigger gaps. If the phase exists, however, it appears already for any $q > 0$, as the synchronisation is much faster for UI.

Our work contributes to the understanding of the necessary conditions for the optimal outcome in coordination games. The study of evolutionary coordination games is well established and had its place in the literature for a long time. Our work also fits into more recent general studies of social systems on multilayer networks. Since many of socio-technical systems have multiple environments where people can interact, the application of layered structures in their modelling is a natural step forward. As we showed, this approach can be highly relevant in analysis of coordination dilemmas, because it leads to non-trivial new effects that have not been observed in single-layer networks.

Methods

We run numerical simulations of the general coordination game defined by the payoff matrix (1) on a multilayer graph. Agents are placed on two networks of N nodes forming two layers of the multilayer network. Each layer is a random regular graph with a degree k , generated using `K-Regular` algorithm from the *igraph* python package^{68,69}. The coupling between layers can be adjusted using two parameters: node overlap q and edge overlap. As we didn't observe any influence of varying edge overlap on the results we maintain a perfect edge overlap, i.e. both layers have exactly the same structure of connections. The node overlap q takes values from 0 to 1, defining the fraction of nodes connected (or shared) between both layers. If two nodes are shared, their state has to be the same on both layers at all times. In other words, it's the same node present on both layers. For $q = 0$ there is no connection between the layers and their dynamics are fully separated, for $q = 1$ it's effectively a single-layer network with each game played half of the time.

The game played on each layer is described by different values of S^β and T^β parameters of the payoff matrix, given in equation (2). We use an asynchronous algorithm where at the beginning of each time step a layer is randomly selected with equal probability for both layers. Then, the update is performed on the chosen layer as for a single-layer network and according to the game played on the layer. First, a random node is chosen with equal probability for all nodes on the layer. We call it the active or focal node. The active node then plays the game with all its k neighbours on the layer and receives a given payoff, which is saved. Finally, the strategy of the active node is updated according to one of the following three update rules:

- the Replicator Dynamics (RD) (aka replicator rule, or proportional imitation rule) – the active node compares the payoff with a random neighbour on the layer and copies its strategy with probability $p = (\text{payoff diff.})/\phi$, if the neighbour's payoff is bigger. Normalisation ϕ is the largest possible payoff difference allowed by the payoff matrix and network structure and it sets the probability p within $[0, 1]$ range,
- the myopic Best Response (BR) – the active node chooses the best strategy given the current strategies of the neighbours on the layer, i.e. it compares all payoffs it would obtain playing each possible strategy against the current strategies of the neighbours and chooses the strategy resulting in the largest payoff,
- the Unconditional Imitation (UI) – the active node copies the strategy of the most successful neighbour on the layer, i.e. the one with the highest payoff, if its payoff is larger.

At the end, the state of the focal node is copied onto the other layer, if the updated node is connected (shared) between the layers. More precisely, the new strategy selected by the node and the last payoff are copied. The simulation runs until a stationary state is reached, or a frozen configuration is obtained on all layers.

References

1. King, A. J., Johnson, D. D. & Van Vugt, M. The origins and evolution of leadership. *Curr. biology* **19**, R911–R916 (2009).
2. Conradt, L. & List, C. Group decisions in humans and animals: a survey. *Philos. transactions The Royal Soc. B: biological sciences* **364**, 719–742 (2009).
3. Courchamp, F., Rasmussen, G. S. & Macdonald, D. W. Small pack size imposes a trade-off between hunting and pup-guarding in the painted hunting dog *lycaon pictus*. *Behav. Ecol.* **13**, 20–27 (2002).
4. Weidenholzer, S. Coordination games and local interactions: a survey of the game theoretic literature. *Games* **1**, 551–585 (2010).
5. Antonioni, A., Cacault, M. P., Lalive, R. & Tomassini, M. Coordination on networks: Does topology matter? *PLoS One* **8**, e55033 (2013).
6. Mazzoli, M. & Sanchez, A. Equilibria, information and frustration in heterogeneous network games with conflicting preferences. *J. Stat. Mech. Theory Exp.* **2017**, 113403 (2017).
7. Antonioni, A., Sanchez, A. & Tomassini, M. Global information and mobility support coordination among humans. *Sci. reports* **4**, 1–7 (2014).
8. Boccaletti, S. *et al.* The structure and dynamics of multilayer networks. *Phys. reports* **544**, 1–122 (2014).
9. Kivelä, M. *et al.* Multilayer networks. *J. complex networks* **2**, 203–271 (2014).
10. Battiston, F., Nicosia, V. & Latora, V. Structural measures for multiplex networks. *Phys. Rev. E* **89**, 032804 (2014).
11. Battiston, F., Nicosia, V. & Latora, V. The new challenges of multiplex networks: Measures and models. *The Eur. Phys. J. Special Top.* **226**, 401–416 (2017).
12. Aleta, A. & Moreno, Y. Multilayer networks in a nutshell. *Annu. Rev. Condens. Matter Phys.* **10**, 45–62 (2019).
13. Gajewski, Ł. G., Chołoniewski, J. & Wilinski, M. Detecting hidden layers from spreading dynamics on complex networks. *Phys. Rev. E* **104**, 024309 (2021).
14. Diakonova, M., Nicosia, V., Latora, V. & San Miguel, M. Irreducibility of multilayer network dynamics: the case of the voter model. *New J. Phys.* **18**, 023010 (2016).
15. Sigmund, K. & Nowak, M. A. Evolutionary game theory. *Curr. Biol.* **9**, R503–R505 (1999).
16. Axelrod, R. & Hamilton, W. D. The evolution of cooperation. *science* **211**, 1390–1396 (1981).
17. Nowak, M. A. & May, R. M. Evolutionary games and spatial chaos. *Nature* **359**, 826–829 (1992).
18. Nowak, M. A. Five rules for the evolution of cooperation. *science* **314**, 1560–1563 (2006).
19. Raducha, T. & San Miguel, M. Coordination and equilibrium selection in games: the role of local effects. *Sci. reports* **12**, 1–16 (2022).
20. Kandori, M., Mailath, G. J. & Rob, R. Learning, mutation, and long run equilibria in games. *Econom. J. Econom. Soc.* 29–56 (1993).
21. Young, H. P. The evolution of conventions. *Econom. J. Econom. Soc.* 57–84 (1993).
22. Young, H. P. *Individual Strategy and Social Structure* (Princeton, Princeton University Press, 1998).
23. Ellison, G. Basins of attraction, long-run stochastic stability, and the speed of step-by-step evolution. *The Rev. Econ. Stud.* **67**, 17–45 (2000).
24. Peski, M. Generalized risk-dominance and asymmetric dynamics. *J. Econ. Theory* **145**, 216–248 (2010).
25. Ellison, G. Learning, local interaction, and coordination. *Econom. J. Econom. Soc.* 1047–1071 (1993).
26. Alós-Ferrer, C. & Weidenholzer, S. Imitation, local interactions, and efficiency. *Econ. Lett.* **93**, 163–168 (2006).
27. Ohtsuki, H. & Nowak, M. A. The replicator equation on graphs. *J. theoretical biology* **243**, 86–97 (2006).
28. Roca, C. P., Cuesta, J. A. & Sánchez, A. Evolutionary game theory: Temporal and spatial effects beyond replicator dynamics. *Phys. life reviews* **6**, 208–249 (2009).
29. Wang, Z., Wang, L., Szolnoki, A. & Perc, M. Evolutionary games on multilayer networks: a colloquium. *The Eur. physical journal B* **88**, 1–15 (2015).
30. Gómez-Gardenes, J., Reinares, I., Arenas, A. & Floría, L. M. Evolution of cooperation in multiplex networks. *Sci. reports* **2**, 1–6 (2012).

31. Matamalas, J. T., Poncela-Casasnovas, J., Gómez, S. & Arenas, A. Strategical incoherence regulates cooperation in social dilemmas on multiplex networks. *Sci. reports* **5**, 1–7 (2015).
32. Wang, Z., Wang, L. & Perc, M. Degree mixing in multilayer networks impedes the evolution of cooperation. *Phys. Rev. E* **89**, 052813 (2014).
33. Amato, R., Díaz-Guilera, A. & Klenkeberg, K.-K. Interplay between social influence and competitive strategical games in multiplex networks. *Sci. reports* **7**, 1–8 (2017).
34. Alós-Ferrer, C. & Weidenholzer, S. Imitation and the role of information in overcoming coordination failures. *Games Econ. Behav.* **87**, 397–411 (2014).
35. Cui, Z. & Wang, R. Collaboration in networks with randomly chosen agents. *J. Econ. Behav. & Organ.* **129**, 129–141 (2016).
36. Khan, A. Coordination under global random interaction and local imitation. *Int. J. Game Theory* **43**, 721–745 (2014).
37. Alós-Ferrer, C., Buckenmaier, J. & Farolfi, F. When are efficient conventions selected in networks? *J. Econ. Dyn. Control.* **124**, 104074 (2021).
38. Tomassini, M. & Antonioni, A. Computational behavioral models in public goods games with migration between groups. *J. Physics: Complex.* **2**, 045013 (2021).
39. Giardini, F., Vilone, D., Sánchez, A. & Antonioni, A. Gossip and competitive altruism support cooperation in a public good game. *Philos. Transactions Royal Soc. B* **376**, 20200303 (2021).
40. Maciel Cardoso, F. *et al.* Framing in multiple public goods games and donation to charities. *Royal Soc. open science* **8**, 202117 (2021).
41. Wang, Z., Szolnoki, A. & Perc, M. Interdependent network reciprocity in evolutionary games. *Sci. reports* **3**, 1–7 (2013).
42. Battiston, F., Perc, M. & Latora, V. Determinants of public cooperation in multiplex networks. *New J. Phys.* **19**, 073017 (2017).
43. Lipari, F., Stella, M. & Antonioni, A. Investigating peer and sorting effects within an adaptive multiplex network model. *Games* **10**, 16 (2019).
44. Lugo, H. & San Miguel, M. Learning and coordinating in a multilayer network. *Sci. reports* **5**, 1–7 (2015).
45. Lugo, H., González-Avella, J. C. & San Miguel, M. Local connectivity effects in learning and coordination dynamics in a two-layer network. *Chaos: An Interdiscip. J. Nonlinear Sci.* **30**, 083125 (2020).
46. González-Avella, J. C., Lugo, H. & San Miguel, M. Coordination in a skeptical two-group population. *J. Econ. Interact. Coord.* **14**, 203–214 (2019).
47. Harsanyi, J. C., Selten, R. *et al.* A general theory of equilibrium selection in games. *MIT Press. Books* **1** (1988).
48. Xia, C. *et al.* Role of update dynamics in the collective cooperation on the spatial snowdrift games: Beyond unconditional imitation and replicator dynamics. *Chaos, Solitons & Fractals* **45**, 1239–1245 (2012).
49. Szolnoki, A. & Danku, Z. Dynamic-sensitive cooperation in the presence of multiple strategy updating rules. *Phys. A: Stat. Mech. its Appl.* **511**, 371–377 (2018).
50. Danku, Z., Wang, Z. & Szolnoki, A. Imitate or innovate: Competition of strategy updating attitudes in spatial social dilemma games. *EPL (Europhysics Lett.)* **121**, 18002 (2018).
51. Poncela-Casasnovas, J. *et al.* Humans display a reduced set of consistent behavioral phenotypes in dyadic games. *Sci. advances* **2**, e1600451 (2016).
52. Szabó, G. & Fath, G. Evolutionary games on graphs. *Phys. reports* **446**, 97–216 (2007).
53. Pangallo, M., Sanders, J. B., Galla, T. & Farmer, J. D. Towards a taxonomy of learning dynamics in 2×2 games. *Games Econ. Behav.* (2021).
54. Blume, L. E. The statistical mechanics of strategic interaction. *Games economic behavior* **5**, 387–424 (1993).
55. Traulsen, A., Pacheco, J. M. & Nowak, M. A. Pairwise comparison and selection temperature in evolutionary game dynamics. *J. theoretical biology* **246**, 522–529 (2007).
56. Schuster, P. & Sigmund, K. Replicator dynamics. *J. theoretical biology* **100**, 533–538 (1983).
57. Hammerstein, P. & Selten, R. Game theory and evolutionary biology. *Handb. game theory with economic applications* **2**, 929–993 (1994).

58. Nowak, M. A. & Sigmund, K. Evolutionary dynamics of biological games. *science* **303**, 793–799 (2004).
59. Blume, L. E. The statistical mechanics of best-response strategy revision. *Games economic behavior* **11**, 111–145 (1995).
60. Sandholm, W. H. Simple and clever decision rules for a model of evolution. *Econ. Lett.* **61**, 165–170 (1998).
61. Buskens, V., Corten, R. & Weesie, J. Consent or conflict: Coevolution of coordination and networks. *J. Peace Res.* **45**, 205–222 (2008).
62. Vilone, D., Ramasco, J. J., Sánchez, A. & San Miguel, M. Social and strategic imitation: the way to consensus. *Sci. reports* **2**, 1–7 (2012).
63. Vilone, D., Ramasco, J. J., Sánchez, A. & San Miguel, M. Social imitation versus strategic choice, or consensus versus cooperation, in the networked prisoner’s dilemma. *Phys. Rev. E* **90**, 022810 (2014).
64. Diakonova, M., San Miguel, M. & Eguiluz, V. M. Absorbing and shattered fragmentation transition in multilayer coevolution. *Phys. Rev. E* **89**, 062818 (2014).
65. Newman, M. *et al.* *Networks: an introduction* (Oxford University Press, 2016).
66. Skyrms, B. The stag hunt. *Proc. Addresses Am. Philos. Assoc.* **75**, 31–41 (2001).
67. Skyrms, B. *The stag hunt and the evolution of social structure* (Cambridge University Press, 2004).
68. Csardi, G., Nepusz, T. *et al.* The igraph software package for complex network research. *InterJournal, complex systems* **1695**, 1–9 (2006).
69. Csardi, G., Nepusz, T. *et al.* igraph Python package. <https://igraph.org/python/>, accessed 2021-12-16.

Acknowledgements

We acknowledge financial support from MCIN/AEI/10.13039/501100011033 and the Fondo Europeo de Desarrollo Regional (FEDER, UE) through project APASOS (PID2021-122256NB-C21) and the María de Maeztu Program for units of Excellence in R&D, grant MDM-2017-0711.

Author contributions statement

M.S.M. and T.R. conceived and designed the research, T.R. conducted the simulations and wrote the initial manuscript, M.S.M. and T.R. analysed the results and reviewed the manuscript.

Competing interests

The authors declare no competing interests.

Additional information

Supplementary information is available for this paper at

Supplementary material for: Multilayer structure enhances the optimal outcome of coordination games

Tomasz Raducha

tjan@math.uc3m.es

Grupo Interdisciplinar de Sistemas Complejos (GISC),

Departamento de Matemáticas, Universidad Carlos III de Madrid, Leganés, Spain

Instituto de Física Interdisciplinar y Sistemas Complejos IFISC (CSIC-UIB), Palma, Spain

Maxi San Miguel

Instituto de Física Interdisciplinar y Sistemas Complejos IFISC (CSIC-UIB), Palma, Spain

In this supplementary material we provide additional plots of coordination rate α for $q = 1$ (as in Figure 2 from the main manuscript), plots of coordination rate α^I and α^{II} on each layer for varying q (as in Figure 3 from the main manuscript), plots of the dependence of q_c on the gap ΔS or ΔT (as in Figure 4 from the main manuscript), and phase diagrams showing the dependence of synchronisation and coordination on q and ΔS or ΔT (as in Figure 6 from the main manuscript). In addition to the cases considered in the main text we show results for *horizontal* and *vertical* cases, which are depicted in Supplementary Figure S1.

For the horizontal case all points lay on the line $T^\beta = -1$ and for the vertical case on $S^\beta = -2$, $\beta \in \{I, II\}$. Since the layers are placed symmetrically around the $T = S + 1$ line, or more precisely around a point (S_0, T_0) at this line, the parameter $\Delta S = S^I - S^{II}$ or $\Delta T = T^I - T^{II}$ is sufficient to determine values of all four parameters S^I, T^I, S^{II}, T^{II} . Namely:

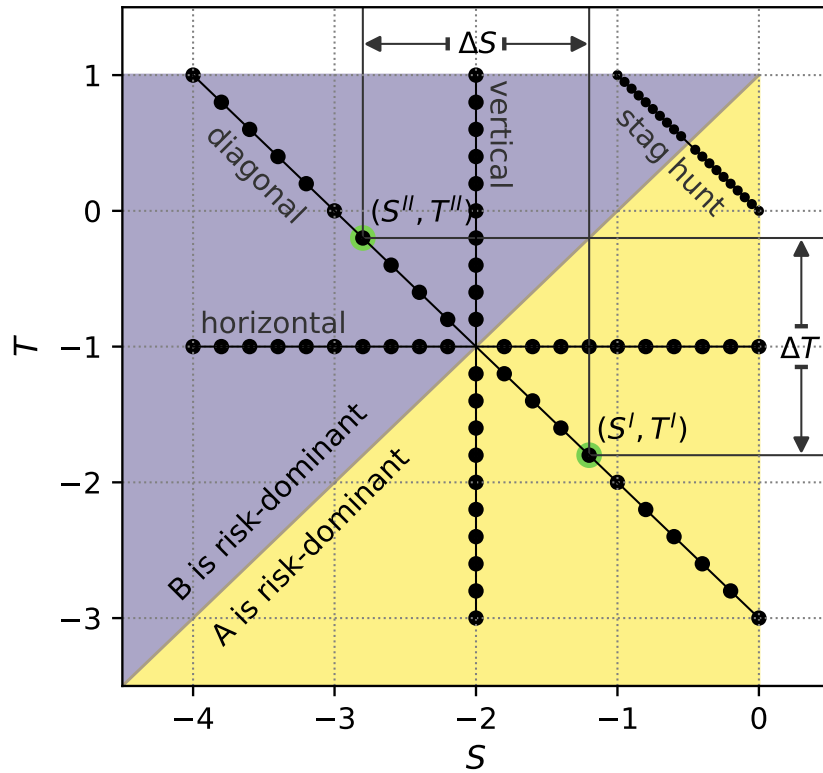
$$\begin{aligned} S_h^I &= S_0 + \frac{\Delta S}{2}, \\ T_h^I &= -1, \\ S_h^{II} &= S_0 - \frac{\Delta S}{2}, \\ T_h^{II} &= -1, \end{aligned} \tag{1}$$

for the horizontal case and:

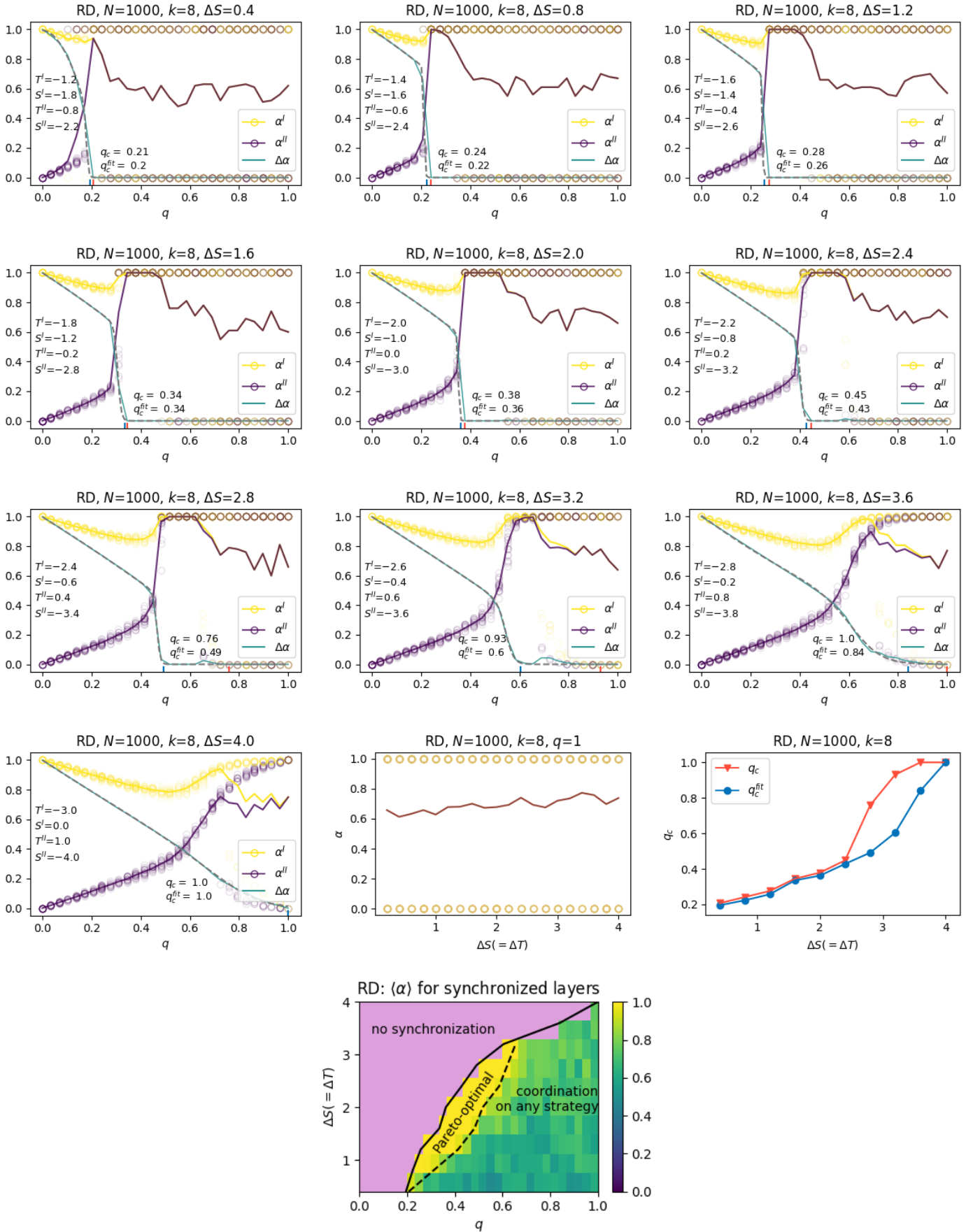
$$\begin{aligned} S_v^I &= -2, \\ T_v^I &= T_0 - \frac{\Delta T}{2}, \\ S_v^{II} &= -2, \\ T_v^{II} &= T_0 + \frac{\Delta T}{2}, \end{aligned} \tag{2}$$

for the vertical case, where $(S_0, T_0) = (-2, -1)$. Note, that horizontal and vertical cases are not fully symmetrical in respect to the games played on the layers. In the horizontal case the game played on layer I has always higher average payoff and in the vertical case the average payoff is bigger on layer II.

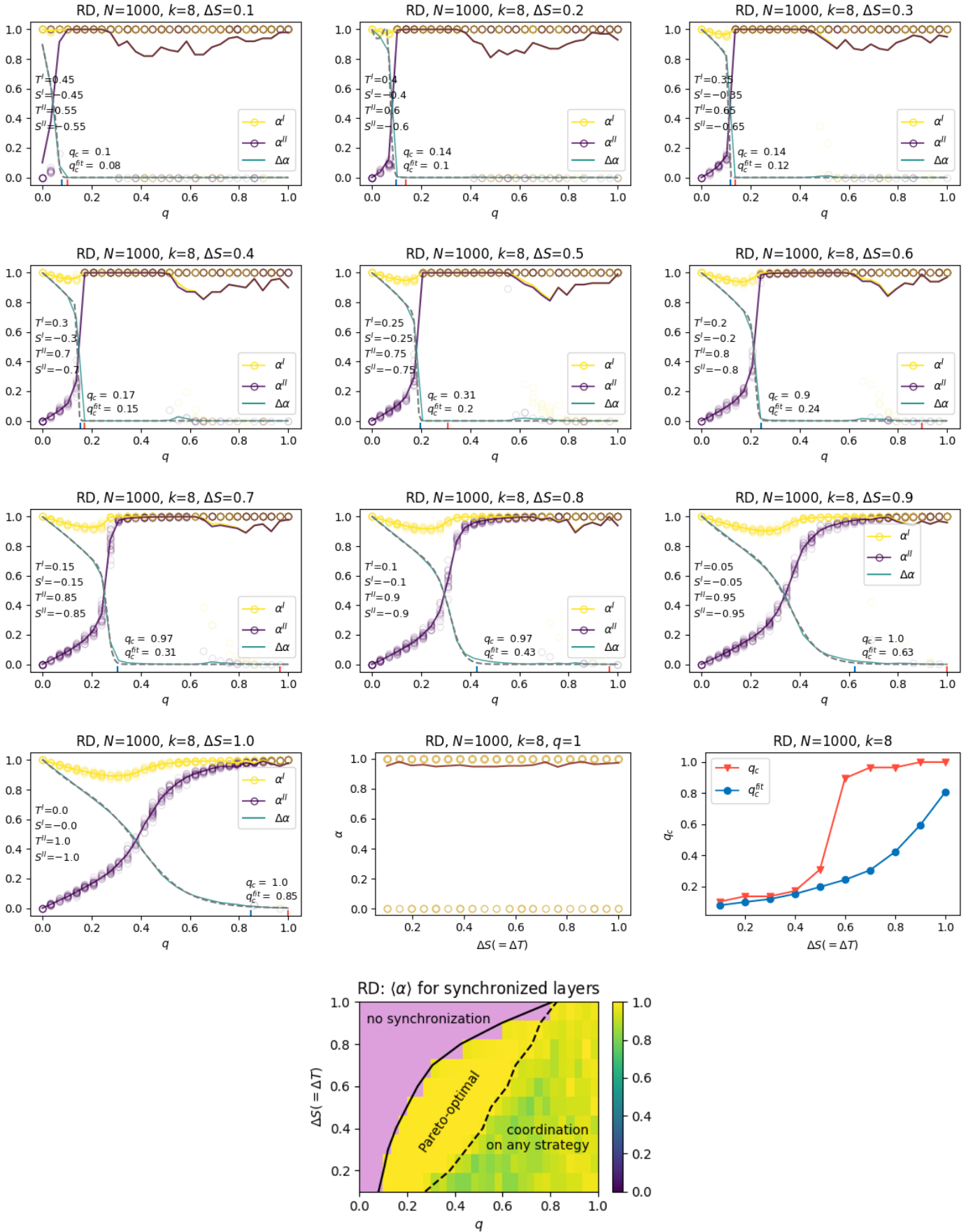
It is worth mentioning that results for BR for higher connectivities indicate that bigger degree may destroy synchronisation (Supplementary Figures S8, S10, and S12). Synchronisation is also weakened in the horizontal case for RD when changing the connectivity from $k = 8$ to a complete graph (Supplementary Figure S5). Additionally, it seems to be detrimental for the Pareto-optimal equilibrium. It is especially interesting, since the Pareto-optimal phase is abundant for UI on a complete graph, except for the vertical case in which the layer II has higher average payoff (Supplementary Figures S14-S17). Finally, the Pareto-optimal phase and synchronisation region are bigger in the vertical case than in the horizontal case for RD (Supplementary Figures S4 and S6). This is especially surprising, because the vertical case is biased towards layer II, as mentioned before, and the horizontal case favours layer I (in terms of the average payoff). The horizontal case results in a bigger Pareto-optimal phase for UI, but surprisingly the effect is inverted for RD.



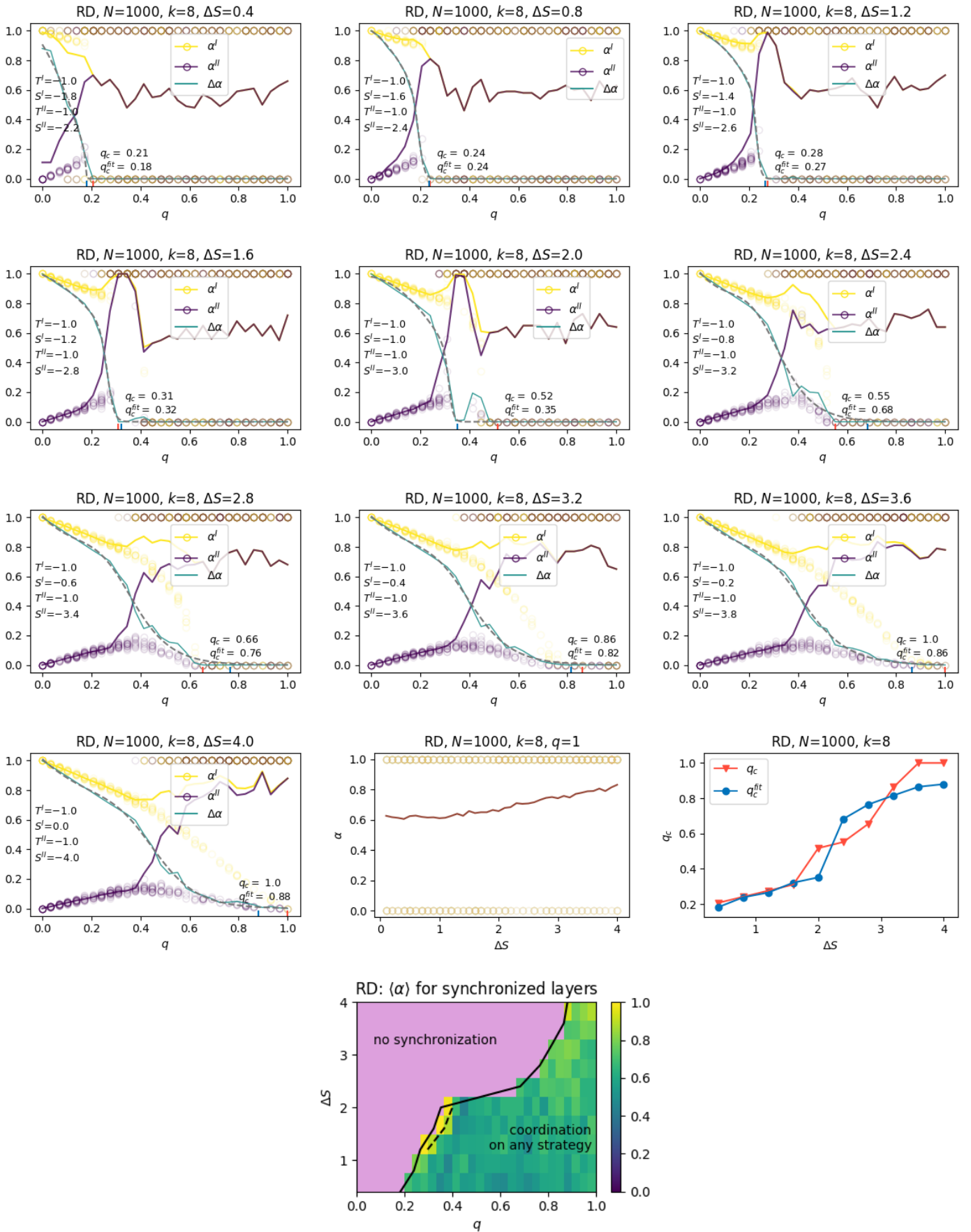
Supplementary Figure S1: Diagram of the S - T parameter space showing parametrisation of the layers. Each circle on the diagonal lines represents a game played on one of the layers. On layer I the strategy A is always risk-dominant (yellow area), and on layer II the strategy B is always risk-dominant (purple area). Risk-dominance changes at the line $T = S + 1$. Exemplary values of (S^I, T^I) and (S^{II}, T^{II}) are highlighted in green with ΔS and ΔT illustrated.



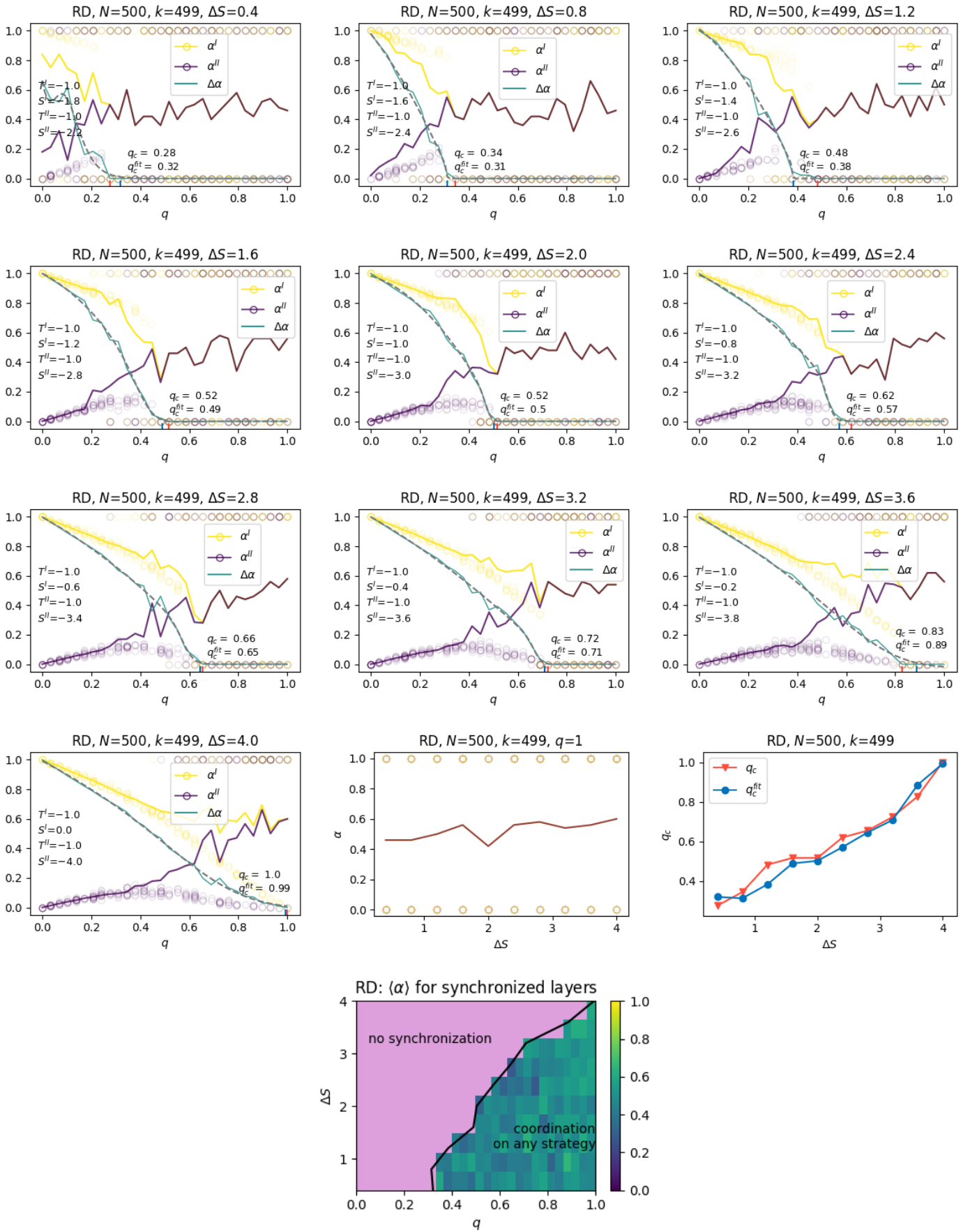
Supplementary Figure S2: **RD in the diagonal case** (i) Coordination rates on layers α^I , α^{II} , and $\Delta\alpha$ vs node overlap q for all values of ΔS . (ii) Coordination rate $\alpha = \alpha^I = \alpha^{II}$ vs gap size ΔS for full node overlap $q = 1$. (iii) Critical value of q_c and q_c^{fit} vs gap size ΔS . (iv) Phase diagram of coordination rate $\alpha = \alpha^I = \alpha^{II}$ in the q - ΔS space for synchronised layers. Each layer has $N = 1000$ nodes with an intra-layer degree $k = 8$. Averaged over (at least) 100 realisations.



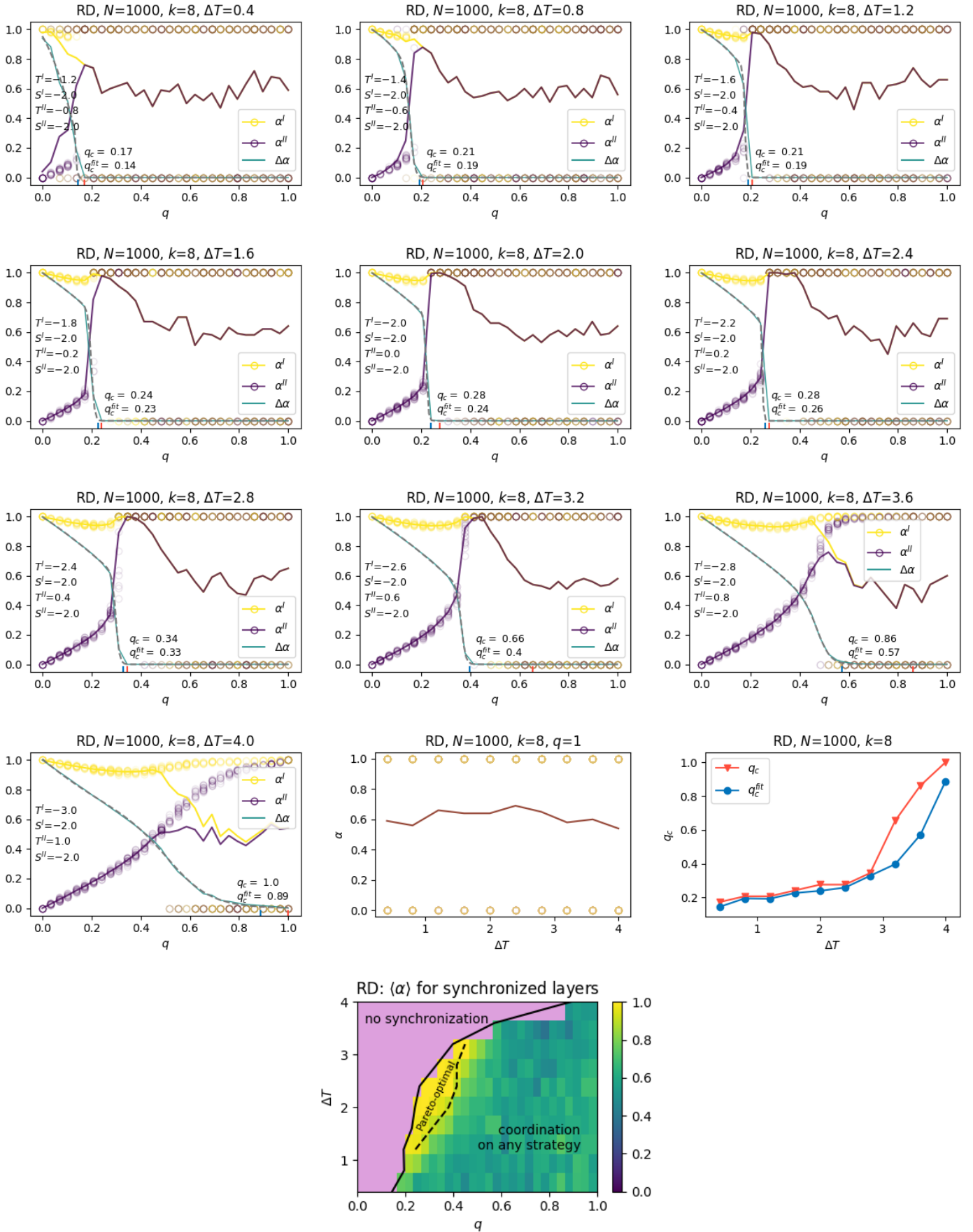
Supplementary Figure S3: **RD in the stag hunt case** (i) Coordination rates on layers α^I , α^{II} , and $\Delta\alpha$ vs node overlap q for all values of ΔS . (ii) Coordination rate $\alpha = \alpha^I = \alpha^{II}$ vs gap size ΔS for full node overlap $q = 1$. (iii) Critical value of q_c and q_c^{fit} vs gap size ΔS . (iv) Phase diagram of coordination rate $\alpha = \alpha^I = \alpha^{II}$ in the q - ΔS space for synchronised layers. Each layer has $N = 1000$ nodes with an intra-layer degree $k = 8$. Averaged over (at least) 100 realisations.



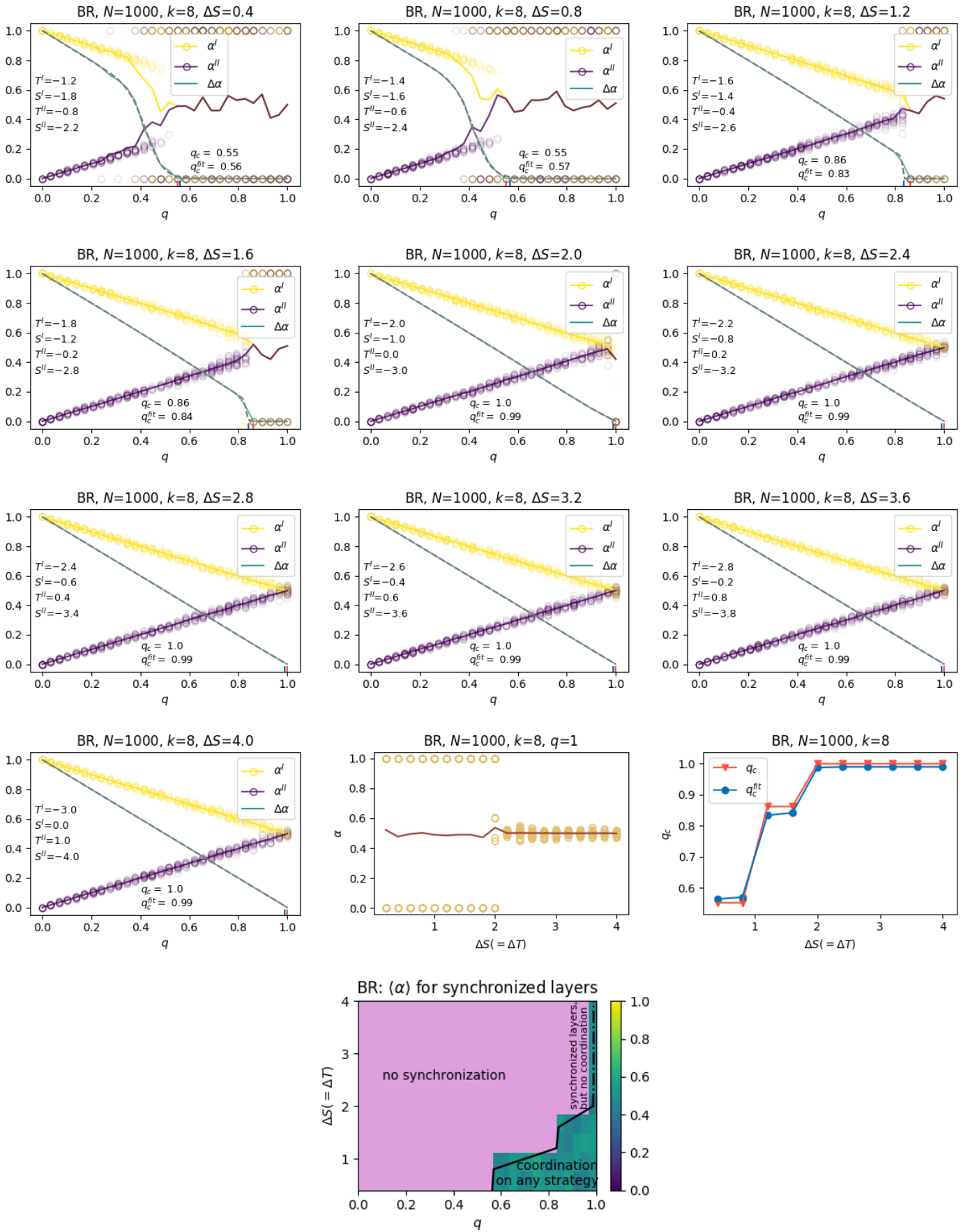
Supplementary Figure S4: **RD in the horizontal case** (i) Coordination rates on layers α^I , α^{II} , and $\Delta\alpha$ vs node overlap q for all values of ΔS . (ii) Coordination rate $\alpha = \alpha^I = \alpha^{II}$ vs gap size ΔS for full node overlap $q = 1$. (iii) Critical value of q_c and q_c^{fit} vs gap size ΔS . (iv) Phase diagram of coordination rate $\alpha = \alpha^I = \alpha^{II}$ in the q - ΔS space for synchronised layers. Each layer has $N = 1000$ nodes with an intra-layer degree $k = 8$. Averaged over (at least) 100 realisations.



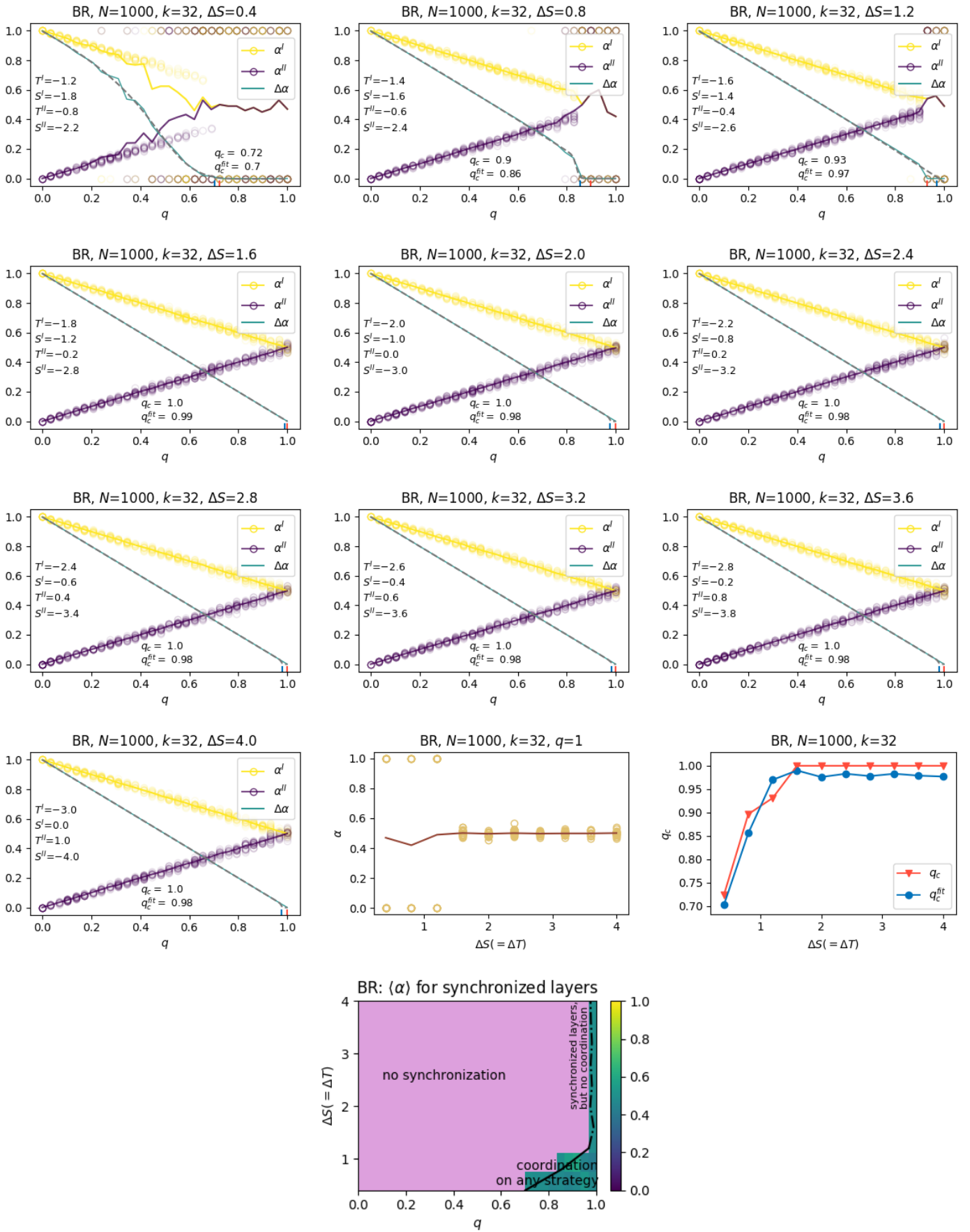
Supplementary Figure S5: **RD in the horizontal case** (i) Coordination rates on layers α^I , α^{II} , and $\Delta\alpha$ vs node overlap q for all values of ΔS . (ii) Coordination rate $\alpha = \alpha^I = \alpha^{II}$ vs gap size ΔS for full node overlap $q = 1$. (iii) Critical value of q_c and q_c^{fit} vs gap size ΔS . (iv) Phase diagram of coordination rate $\alpha = \alpha^I = \alpha^{II}$ in the q - ΔS space for synchronised layers. Each layer has $N = 500$ nodes and forms a complete graph. Averaged over (at least) 50 realisations.



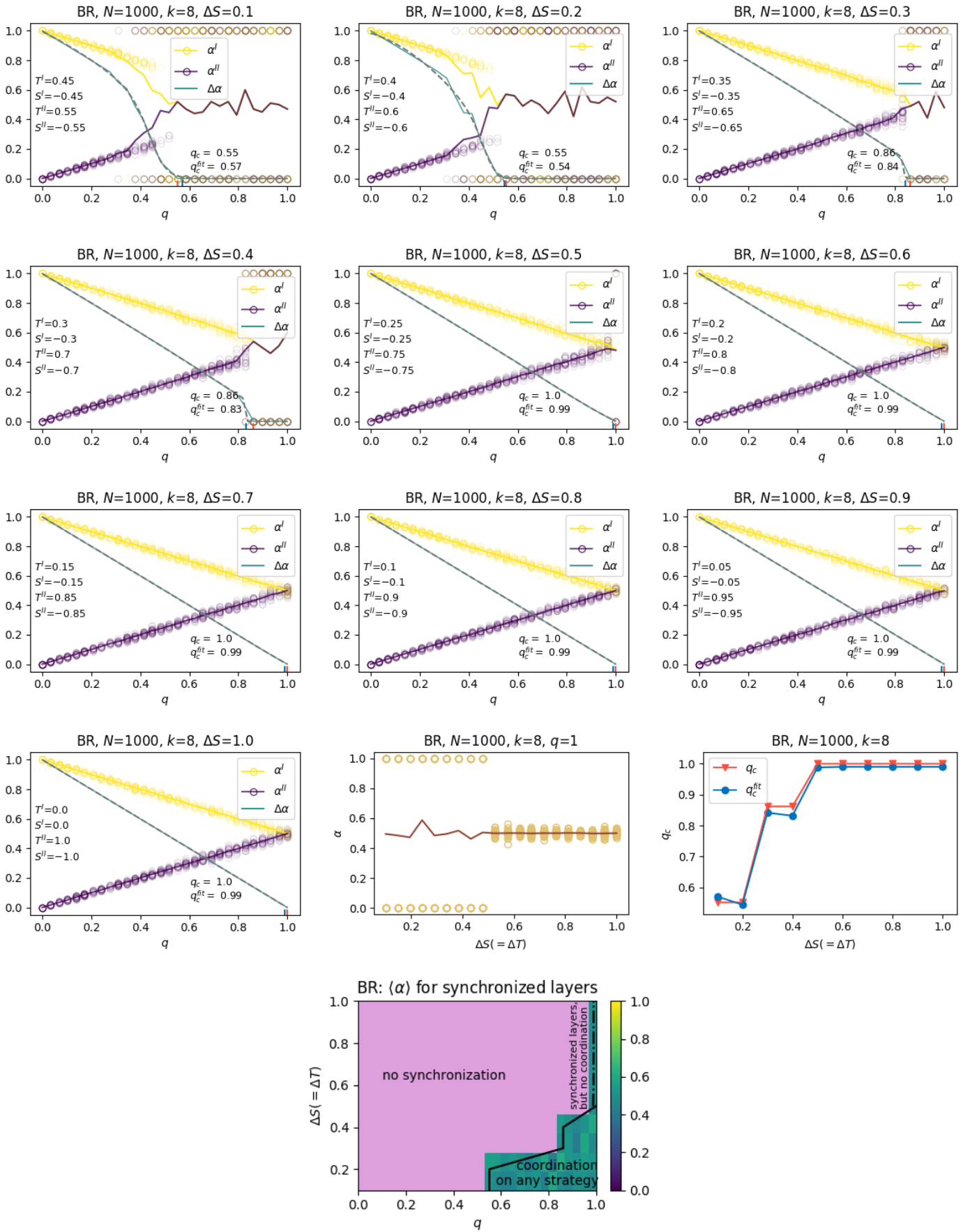
Supplementary Figure S6: **RD in the vertical case** (i) Coordination rates on layers α^I , α^{II} , and $\Delta\alpha$ vs node overlap q for all values of ΔT . (ii) Coordination rate $\alpha = \alpha^I = \alpha^{II}$ vs gap size ΔT for full node overlap $q = 1$. (iii) Critical value of q_c and q_c^{fit} vs gap size ΔT . (iv) Phase diagram of coordination rate $\alpha = \alpha^I = \alpha^{II}$ in the q - ΔT space for synchronised layers. Each layer has $N = 1000$ nodes with an intra-layer degree $k = 8$. Averaged over (at least) 100 realisations.



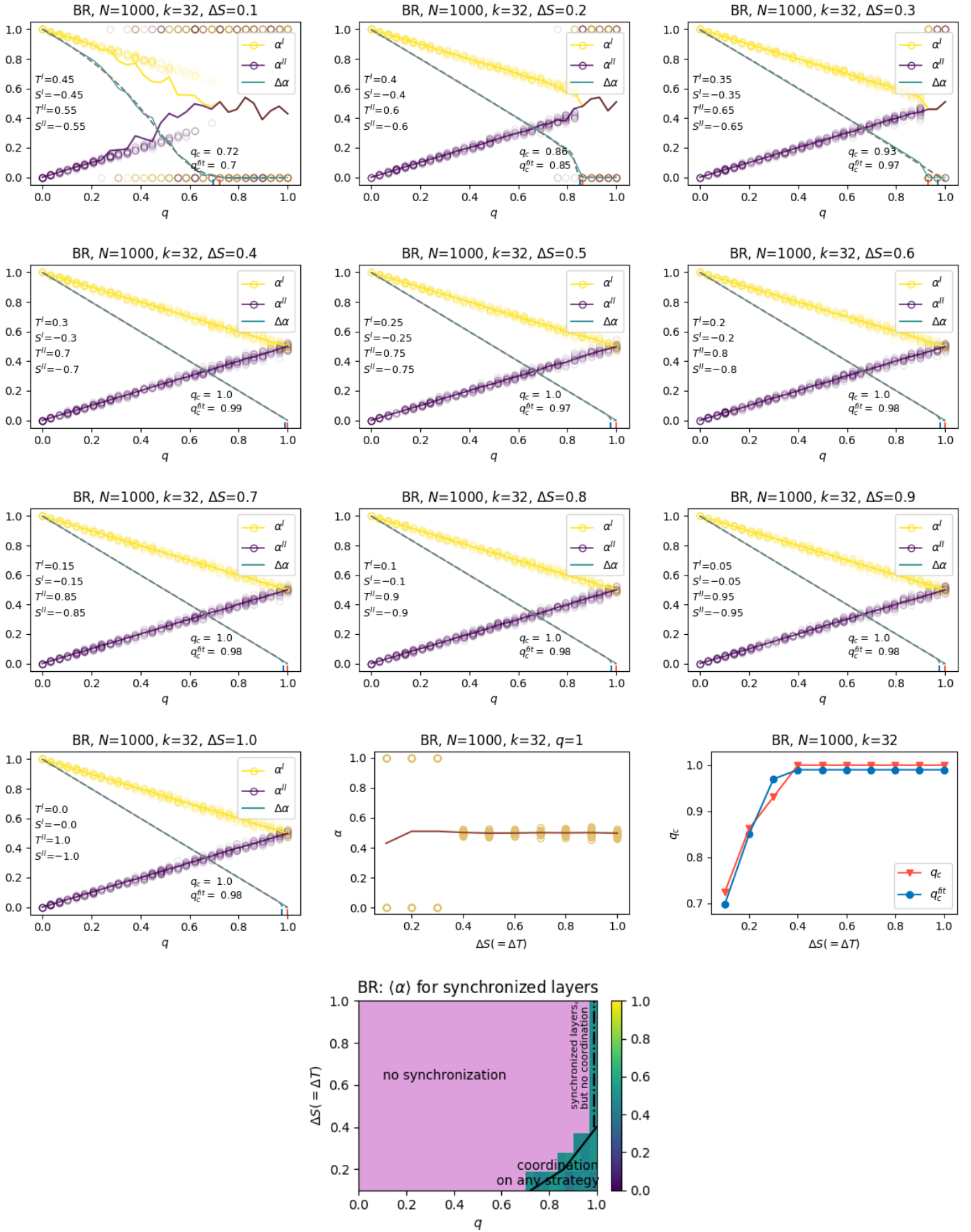
Supplementary Figure S7: **BR in the diagonal case** (i) Coordination rates on layers α^I , α^{II} , and $\Delta\alpha$ vs node overlap q for all values of ΔS . (ii) Coordination rate $\alpha = \alpha^I = \alpha^{II}$ vs gap size ΔS for full node overlap $q = 1$. (iii) Critical value of q_c and q_c^{fit} vs gap size ΔS . (iv) Phase diagram of coordination rate $\alpha = \alpha^I = \alpha^{II}$ in the q - ΔS space for synchronised layers. Each layer has $N = 1000$ nodes with an intra-layer degree $k = 8$. Averaged over (at least) 100 realisations.



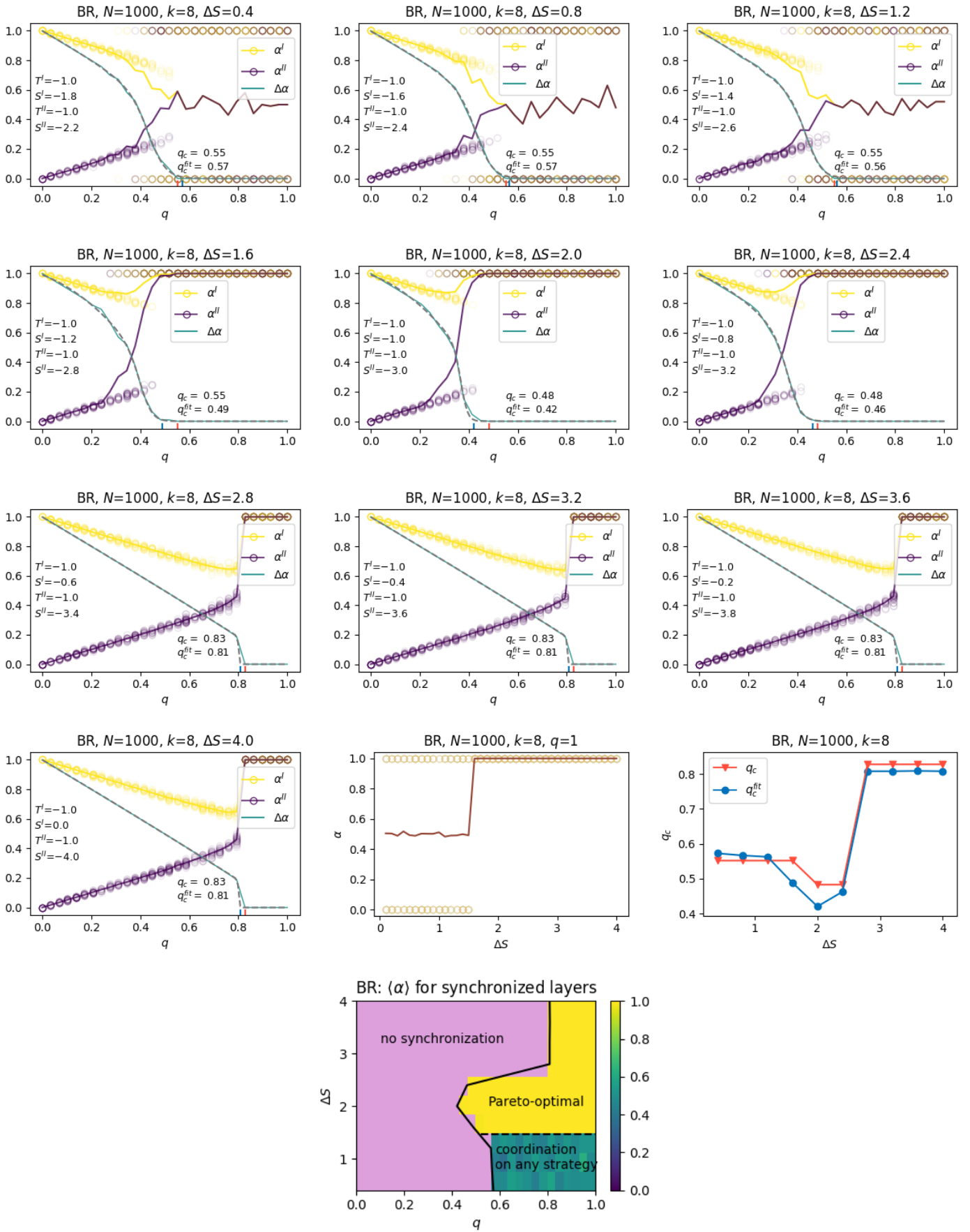
Supplementary Figure S8: **BR in the diagonal case** (i) Coordination rates on layers α^I , α^{II} , and $\Delta\alpha$ vs node overlap q for all values of ΔS . (ii) Coordination rate $\alpha = \alpha^I = \alpha^{II}$ vs gap size ΔS for full node overlap $q = 1$. (iii) Critical value of q_c and q_c^{fit} vs gap size ΔS . (iv) Phase diagram of coordination rate $\alpha = \alpha^I = \alpha^{II}$ in the q - ΔS space for synchronised layers. Each layer has $N = 1000$ nodes with an intra-layer degree $k = 32$. Averaged over (at least) 100 realisations.



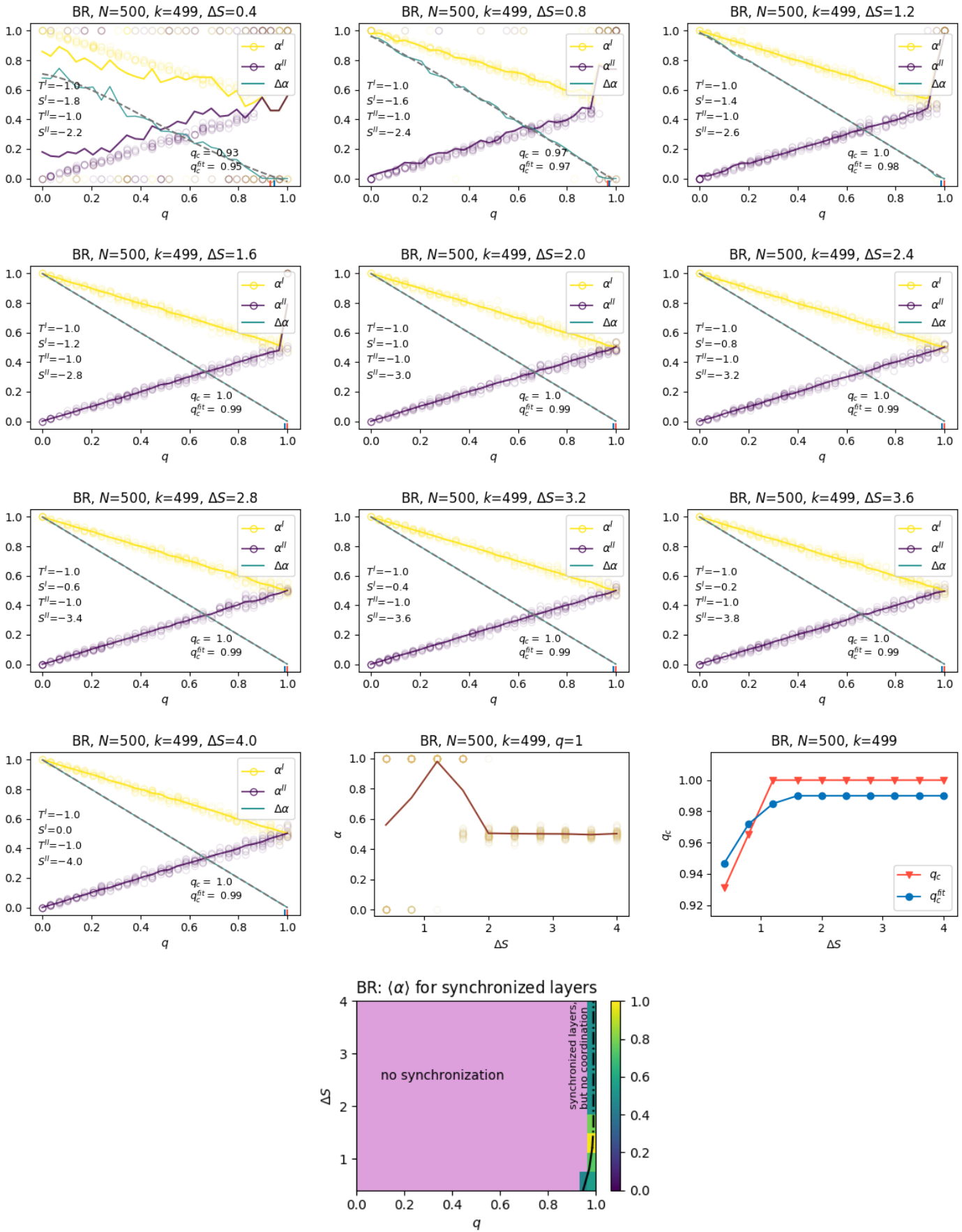
Supplementary Figure S9: **BR in the stag hunt case** (i) Coordination rates on layers α^I , α^{II} , and $\Delta\alpha$ vs node overlap q for all values of ΔS . (ii) Coordination rate $\alpha = \alpha^I = \alpha^{II}$ vs gap size ΔS for full node overlap $q = 1$. (iii) Critical value of q_c and q_c^{fit} vs gap size ΔS . (iv) Phase diagram of coordination rate $\alpha = \alpha^I = \alpha^{II}$ in the q - ΔS space for synchronised layers. Each layer has $N = 1000$ nodes with an intra-layer degree $k = 8$. Averaged over (at least) 100 realisations.



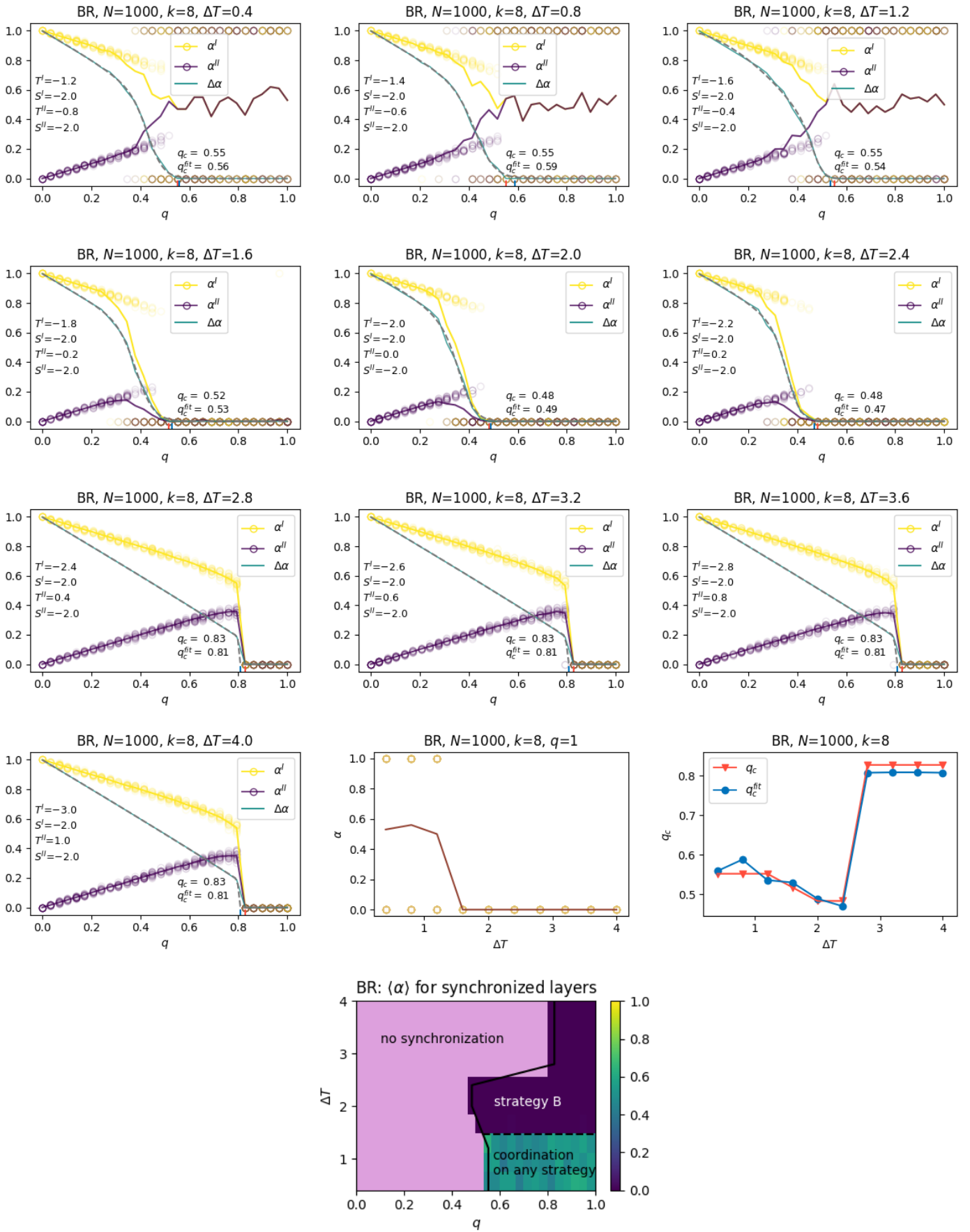
Supplementary Figure S10: **BR in the stag hunt case** (i) Coordination rates on layers α^I , α^{II} , and $\Delta\alpha$ vs node overlap q for all values of ΔS . (ii) Coordination rate $\alpha = \alpha^I = \alpha^{II}$ vs gap size ΔS for full node overlap $q = 1$. (iii) Critical value of q_c and q_c^{fit} vs gap size ΔS . (iv) Phase diagram of coordination rate $\alpha = \alpha^I = \alpha^{II}$ in the q - ΔS space for synchronised layers. Each layer has $N = 1000$ nodes with an intra-layer degree $k = 32$. Averaged over (at least) 100 realisations.



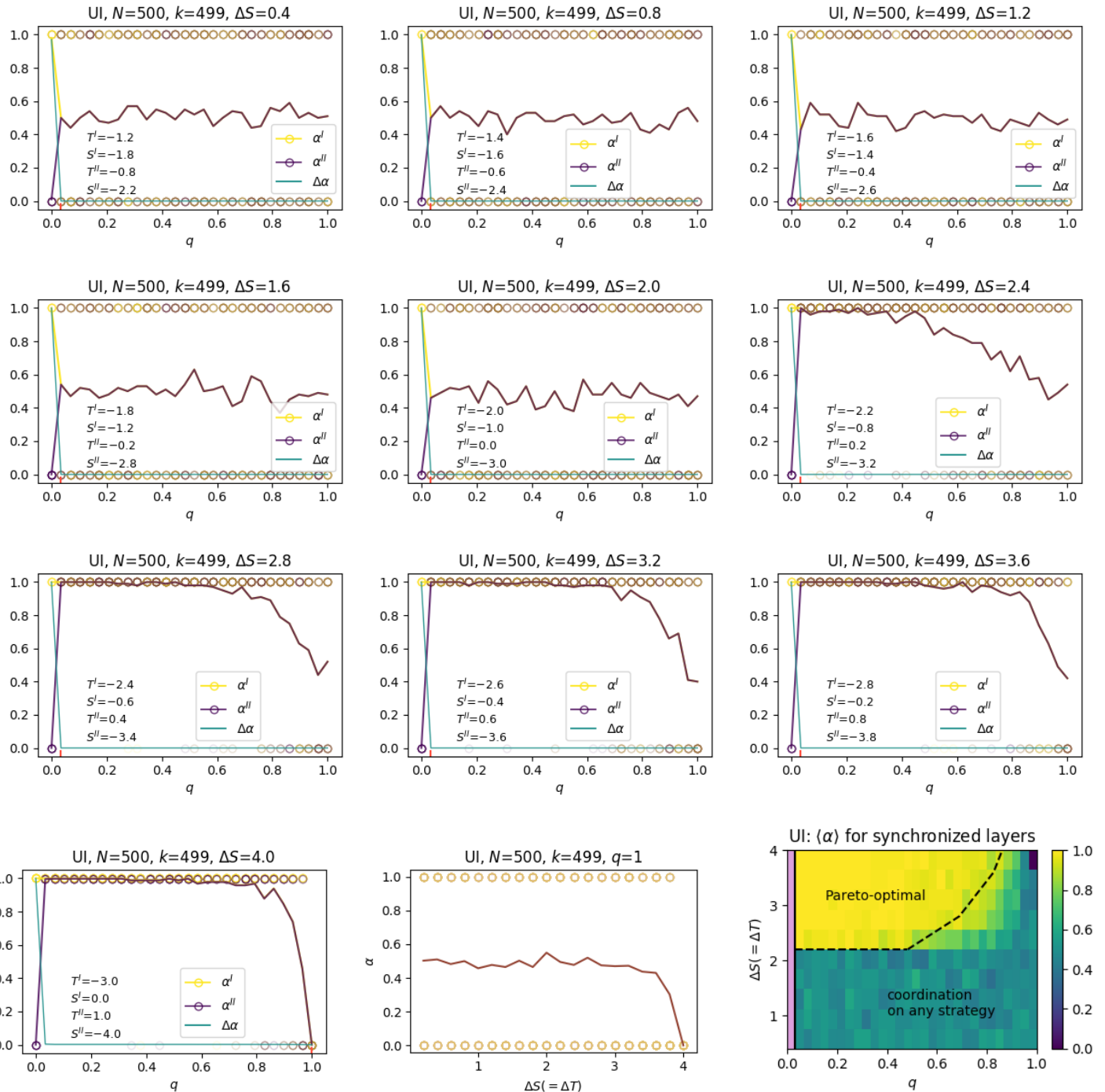
Supplementary Figure S11: **BR in the horizontal case** (i) Coordination rates on layers α^I , α^{II} , and $\Delta\alpha$ vs node overlap q for all values of ΔS . (ii) Coordination rate $\alpha = \alpha^I = \alpha^{II}$ vs gap size ΔS for full node overlap $q = 1$. (iii) Critical value of q_c and q_c^{fit} vs gap size ΔS . (iv) Phase diagram of coordination rate $\alpha = \alpha^I = \alpha^{II}$ in the q - ΔS space for synchronised layers. Each layer has $N = 1000$ nodes with an intra-layer degree $k = 8$. Averaged over (at least) 100 realisations.



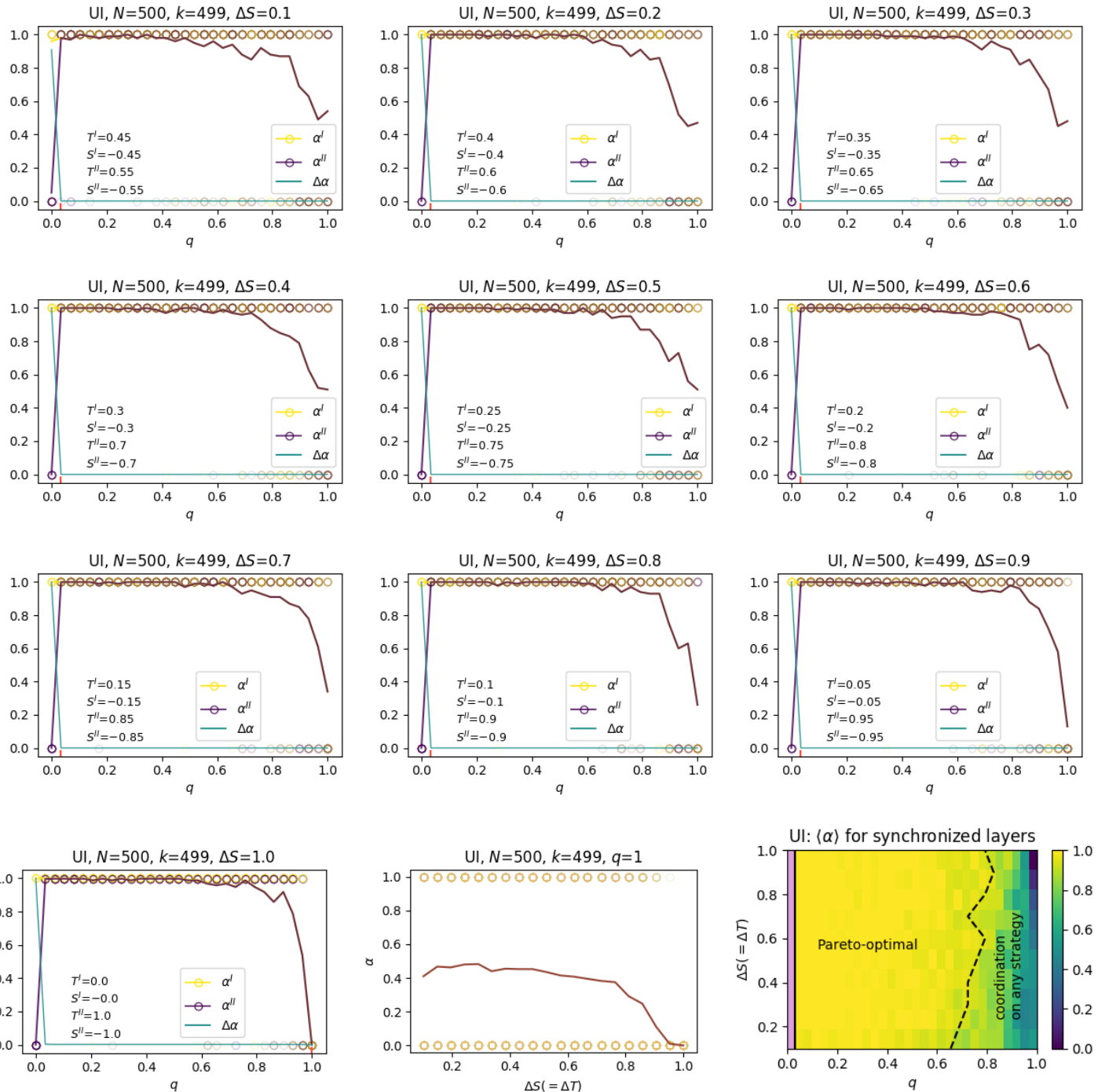
Supplementary Figure S12: **BR in the horizontal case** (i) Coordination rates on layers α^I , α^{II} , and $\Delta\alpha$ vs node overlap q for all values of ΔS . (ii) Coordination rate $\alpha = \alpha^I = \alpha^{II}$ vs gap size ΔS for full node overlap $q = 1$. (iii) Critical value of q_c and q_c^{fit} vs gap size ΔS . (iv) Phase diagram of coordination rate $\alpha = \alpha^I = \alpha^{II}$ in the q - ΔS space for synchronised layers. Each layer has $N = 500$ nodes and forms a complete graph. Averaged over (at least) 50 realisations.



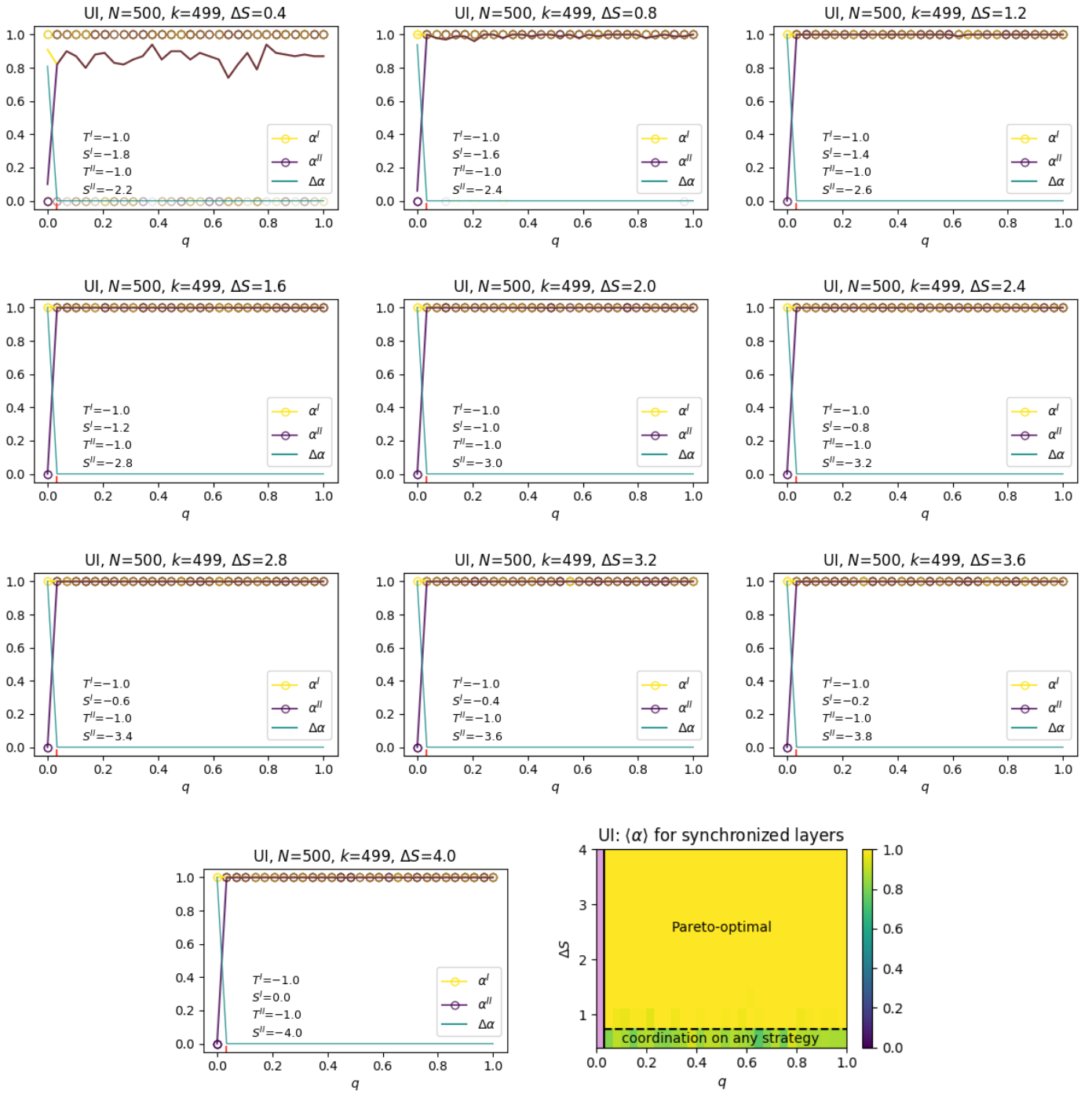
Supplementary Figure S13: **BR in the vertical case** (i) Coordination rates on layers α^I , α^{II} , and $\Delta\alpha$ vs node overlap q for all values of ΔT . (ii) Coordination rate $\alpha = \alpha^I = \alpha^{II}$ vs gap size ΔT for full node overlap $q = 1$. (iii) Critical value of q_c and q_c^{fit} vs gap size ΔT . (iv) Phase diagram of coordination rate $\alpha = \alpha^I = \alpha^{II}$ in the q - ΔT space for synchronised layers. Each layer has $N = 1000$ nodes with an intra-layer degree $k = 8$. Averaged over (at least) 100 realisations.



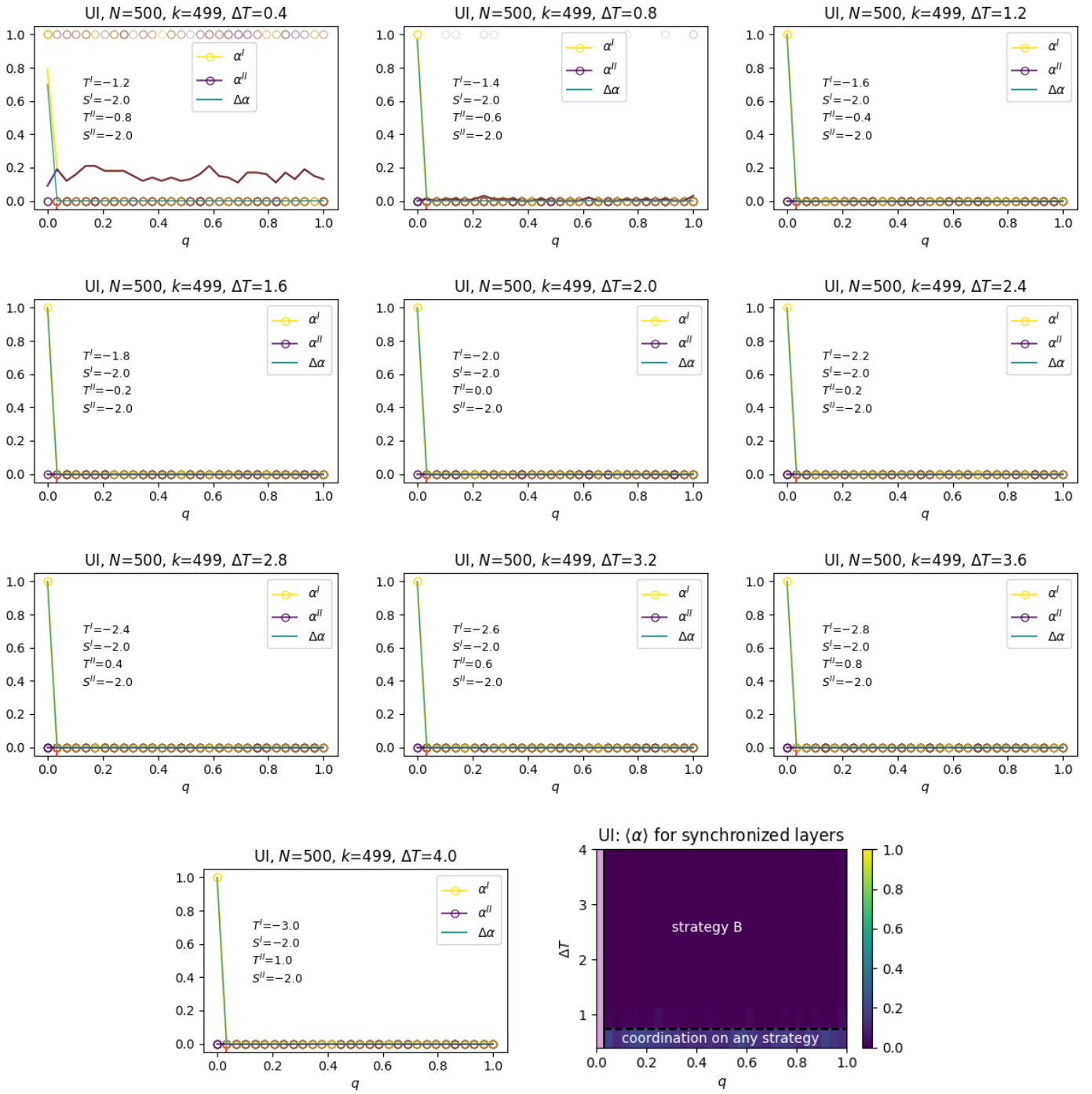
Supplementary Figure S14: **UI in the diagonal case** (i) Coordination rates on layers α^I , α^{II} , and $\Delta\alpha$ vs node overlap q for all values of ΔS . (ii) Coordination rate $\alpha = \alpha^I = \alpha^{II}$ vs gap size ΔS for full node overlap $q = 1$. (iii) Phase diagram of coordination rate $\alpha = \alpha^I = \alpha^{II}$ in the q - ΔS space for synchronised layers. Each layer has $N = 1000$ nodes and forms a complete graph. Averaged over (at least) 100 realisations.



Supplementary Figure S15: **UI in the stag hunt case** (i) Coordination rates on layers α^I , α^{II} , and $\Delta\alpha$ vs node overlap q for all values of ΔS . (ii) Coordination rate $\alpha = \alpha^I = \alpha^{II}$ vs gap size ΔS for full node overlap $q = 1$. (iii) Phase diagram of coordination rate $\alpha = \alpha^I = \alpha^{II}$ in the $q - \Delta S$ space for synchronised layers. Each layer has $N = 1000$ nodes and forms a complete graph. Averaged over (at least) 100 realisations.



Supplementary Figure S16: **UI in the horizontal case** (i) Coordination rates on layers α^I , α^{II} , and $\Delta\alpha$ vs node overlap q for all values of ΔS . (ii) Phase diagram of coordination rate $\alpha = \alpha^I = \alpha^{II}$ in the q - ΔS space for synchronised layers. Each layer has $N = 1000$ nodes and forms a complete graph. Averaged over (at least) 100 realisations.



Supplementary Figure S17: **UI in the vertical case** (i) Coordination rates on layers α^I , α^{II} , and $\Delta\alpha$ vs node overlap q for all values of ΔT . (ii) Phase diagram of coordination rate $\alpha = \alpha^I = \alpha^{II}$ in the q - ΔT space for synchronised layers. Each layer has $N = 1000$ nodes and forms a complete graph. Averaged over (at least) 100 realisations.